UNIVERSITY OF CALIFORNIA, SAN DIEGO

Mutant Protein Tyrosine Phosphatase Non-Receptor Type 2 Increases Permeability of Intestinal Epithelial Barrier Function

A thesis submitted in partial satisfaction of the

requirements for the degree Master of Science

in

Biology

by

Taylaur W. Smith

Committee in charge:

Professor Kim E. Barrett, Chair
Professor David S. Woodruff, Co-Chair
Professor Declan F. McCole
Professor Kit J. Pogliano

2012

The Thesis of Taylaur W. Smith is approved and is acceptable in quality and in form for publication on microfilm and electronically:

Co-Chair

Chair

University of California, San Diego

2012

TABLE OF CONTENTS

LIST OF FIGURES

LIST OF TABLES

ACKNOWLEDGEMENTS

I would like to first express my gratitude for Dr. Kim Barrett and Dr. Declan McCole for their guidance over the past two years. I have learned an immeasurable amount from both of them. This is not only in relation to lab but also within the professional world. I am confident that the knowledge that I have gained will follow me through everything that is to come. Thank you for all of your kindness and support over the years.

I would also like to thank Dr. David Woodruff and Dr. Kit Pogliano for serving as members on my committee.

I am extremely indebted to Dr. Ronald Marchelletta who worked side by side with me throughout the project and was always willing to step in when it was needed. Ron demonstrated his patience countless times in teaching me all of the techniques he possibly could out of the kindness of his heart. He works hard to make the lab a welcoming place for all of the students that stopped by. I would also like to acknowledge that Dr. Marchelletta is co-author for material included in Figures 17 and 18 that will be prepared for publication.

To my parents, Doug and Laura, who have supported me in everything I do, thank you. I truly would not have accomplished everything I have without them. I would like to thank Bailey for being a wonderful role model and consistently making me strive to be better. And, of course, Carli who has put her own sweat and tears into this project. Without her, this project and my thesis would not have been completed. I love you all.

Finally, my friends, particularly Nicholas Placone, I would like to apologize and thank them for dealing with me throughout the ups and downs that accompany research.

ABSTRACT OF THE THESIS

Mutant Protein Tyrosine Phosphatase Non-Receptor Type 2 Increases Intestinal Epithelial Permeability

by

Taylaur W. Smith

Master of Science in Biology

University of California, San Diego, 2012

Professor Kim E. Barrett, Chair
Professor David S. Woodruff, Co-Chair

Mutations in Protein Tyrosine-Phosphatase Non-Receptor Type 2 (PTPN2) were found by Genome-Wide Association Studies (GWAS) to be associated with the onset and progression of the chronic intestinal inflammatory conditions, Crohn's disease and ulcerative colitis, collectively known as Inflammatory Bowel Disease (IBD). PTPN2 negatively regulates signaling pathways induced by the pro-inflammatory cytokine

interferon-gamma (IFN-γ). IFN-γ is clinically important due to its critical role in IBD pathogenesis, which includes increasing permeability of the intestinal epithelial lining. A recent study by our laboratory demonstrated that PTPN2 knock-down in intestinal epithelial cells permits enhanced signaling by IFN-γ, and increased permeability of epithelial monolayers. Specifically, increased phosphorylation of downstream signaling targets such as signal transducer and activator of transcription-1 (STAT1) was observed, accompanied by enhanced expression of an IBD-associated pore-forming protein, claudin-2 (CLD2), that increases epithelial barrier permeability.

Here, I detail the production of a cell line that stably expresses dominant-negative TC45 (a splice-variant of PTPN2) via lentiviral transduction, in order to better evaluate the consequences of dysfunctional PTPN2 regulation. I observed trafficking disturbances in the TC45 mutant potentially providing an explanation for dysregulation of PTPN2 and its link to barrier dysfunction. My results support earlier findings of increased phosphorylated STAT1 and subsequent increase in CLD-2. The cell line also displays a concurrent decrease in matriptase-1, a protease responsible for rapid turnover of CLD-2, indicating that this normally protective pathway is TC45-dependent. These studies offer new insights into the mechanisms through which PTPN2 mutations may explain in part the pathophysiological features of chronic IBD.

I. INTRODUCTION

Gastrointestinal Epithelial Barrier

The lumen of the digestive system is lined by a single layer of epithelial cells. This cellular monolayer forms a selective barrier that allows the digestive system to perform crucial functions including absorption of water and nutrients, maintaining ionic homeostasis, and establishing a protective layer between the intestinal flora and the sub-mucosa [1]

The intestinal epithelial barrier is critical for proper gastrointestinal function and homeostasis. Disrupted barrier function can lead or contribute to many acute and chronic inflammatory or infectious intestinal conditions [2]. For example, a major inflammatory symptom in many patients afflicted with Inflammatory Bowel Disease (IBD) is diarrhea, which can be caused in part by a loss of the integrity of this epithelial barrier [3, 4]. This dysfunction of the intestinal barrier, along with an inappropriate immune response to commensal flora, aids in the development of chronic intestinal inflammation [1, 5].

Inflammatory Bowel Disease

IBD encompasses two chronic conditions of the gastrointestinal tract: Crohn's disease (CD) and ulcerative colitis (UC) [1]. Prevalence of IBD varies greatly depending on geographic region. In areas of high incidence such as North America, both UC and CD have prevalence ranges from 30 to 250 per 100,000 persons[6]. When extrapolated to include an estimated North American population of 320 million in 2003, approximately 780,000 people were afflicted with UC and upwards of 630,000 people suffered from CD [6]. The pathogenesis of both subtypes of IBD is a multi-factorial [7]. Factors that have

been identified as contributing to the progression of disease include genetic predisposition, environmental triggers, and an inappropriate immune response to normally harmless commensal flora in the gut [7]. UC and CD however differ from each other by anatomic distribution and types of ulcerations [1]. UC presents with superficial ulcerations confined to the colon whereas CD is known to affect all regions along the gastrointestinal tract with deep, penetrating lesions [5].

Pro-inflammatory cytokines secreted by immune cells play an important role in the pathogenesis of both conditions but they also serve to differentiate these two diseases [8]. The cytokines interleukin-13 (IL-13) and interferon-γ (IFN-γ) are elevated at the onset of UC and CD, respectively [9]. Increased IFN-γ is linked to CD due to an overactive T-cell response, particularly by a helper T-cell subpopulation, T_H1. Antigen-presenting cells in the mucosa of the gut trigger the activation of T_H1 cells, which in turn, produce and secrete IFN-γ [9]. Overstimulation of a T_H1 immune response results in high concentrations of IFN-γ that have been found to be associated with Crohn's disease [8, 9].

The presence of cytokines, including IFN-γ and tumor necrosis factor-α (TNF-α), has been found to decrease epithelial barrier function reflected by increased permeability and decreased resistance of the intestinal epithelium [1]. Cytokines are implicated in facilitating increases in permeability by both pore and leak pathways. The pore pathway occurs as a result of increased expression and localization of pore-forming proteins, such as Claudin-2, to the tight junctions of the cellular monolayer. The leak pathway, strongly associated with increases in TNF-α and IFN-γ activity, involves a simultaneous contraction of an actinomyosin "belt" coupled with internalization of components of the

tight-junction such as junctional adhesion molecule A (JAM-A) [1, 10]. Constricting the cell while loosening the extracellular constituents that maintain the tight junction, leads to breaches between adjacent epithelial cells that form the barrier [1]. Barrier function and integrity are resolved when there are decreased pro-inflammatory cytokine concentrations and increased activity of negative regulators of these cytokine-signaling pathways.

The role of PTPN2 and mutations associated with CD

A negative regulator of IFN-γ signaling is protein tyrosine phosphatase non-receptor type 2 (PTPN2) [11]. Our group has previously identified a completely novel role for the PTPN2 gene, and its protein product T-cell protein tyrosine phosphatase (TCPTP), in the protection of epithelial barrier function from the effects of IFN-γ. Knockdown of TCPTP expression enhanced the ability of IFN-γ to induce barrier defects by than seen in TCPTP-expressing cells. Furthermore, this increase in permeability was associated with increased expression of the pore-forming tight junction protein, claudin-2 even though IFN-γ does not induce claudin-2 expression in TCPTP-replete cells. These studies provided the rationale for the investigations described herein. PTPN2 is a member of a large family of protein tyrosine phosphatases that share a conserved catalytic domain. Phosphatases function counter to kinases to cleave phosphate groups from tyrosine residues on target proteins as part of an important signaling event. The protein product of the PTPN2 gene, TCPTP, is crucial in the cellular function of a variety of cell types, such as epithelial and hematopoietic cells [12].

Epidermal Growth Factor Receptor and Insulin Receptors are among some of the established substrates of PTPN2. PTPN2 is also known to negatively regulate IFN-γ

receptor (IFN-γR) and its downstream targeting molecules, signal transducers and activators of transcription (STATs), that are phosphorylated upon activation of the IFN-γ receptor [13-15]. As illustrated by Figure 1, IFN-γ binds its receptor causing dimerization and phosphorylation of the receptor via JAK kinase. Phosphorylation of IFN-γR tails leads to the recruitment of STATs that subsequently get phosphorylated and activated. Activated STATs form dimers thereby exposing their nuclear localization signals permitting translocation into the nucleus where they act to upregulate transcription of target genes [16].

TCPTP exists in two main splice variants of 45-kilodalton and 48-kilodalton [17]. The 48KD form (TC48) contains an ER localization signal at the N-terminus and, thus, localizes to the endoplasmic reticulum (ER). The 45KD variant, however, loses the ER localization signal and it is replaced with a nuclear importation signal that permits shuttling from the cytosol to the nucleus [17]. The 45KD variant (TC45) is the primary phosphatase for STATs, particularly STATs 1, 3 and 9, [17-19]. STAT dephosphorylation leads to inactivation and termination of STAT-mediated transcription [17].

Multiple genome-wide-association-studies (GWAS) have shown that individuals with single nucleotide polymorphic (SNP) mutations in the PTPN2 gene have an increased risk of developing CD and UC, thus implicating PTPN2 in the etiology of IBD [11]. PTPN2 knock-out mice develop hematopoietic defects, diarrhea, anemia and only survive for 3-5 weeks due to systemic inflammation, thereby demonstrating the necessity of PTPN2 for overall survival [20]. Furthermore, bone marrow chimeric studies identified that loss of PTPN2 in non-hematopoietic cells is the key factor in the observed

pathology [20]. These studies serve to emphasize the importance of PTPN2 (TCPTP) in regulating inflammation.

Development of a dominant-negative model of PTPN2 dysfunction

Past studies with PTPN2 knock downs using small interfering RNA have demonstrated the regulatory effect of PTPN2 on the STAT1 pathway [3]. However, the direct link between mutations in PTPN2 and their effect on PTPN2 dysfunction remain unknown. In order to explore the effect of PTPN2 mutations on the barrier function of an epithelial monolayer, two TC45 mutants were developed. One is an active-site mutation that alters the critical cysteine residue Cys216 to Ser216 ($TC45^{C216S}$), and the other is a frameshift mutation at Asp206, which models the single-nucleotide polymorphism (SNP) rs34387614 ($TC45^{N206\text{-}fs}$). Both of these mutations are seen on Figure 2. This SNP is a loss-of-function mutation that has been detected in humans but remains uncharacterized in CD.

I aimed to study the effect of TC45 loss-of-function mutants on phosphorylation, and thus activation, of STAT1 as well as expression and localization of a potential STAT1 target gene, claudin-2. The location and amount of the pore-forming claudin-2 protein was expected to provide insights into the precise mechanism by which TC45 defects play a role in exacerbated leakage through the epithelial barrier.

Previous studies also indicated a specific protease, matriptase-1 (MAT1), is responsible for the rapid turnover of claudin-2 at the tight junctions [21, 22]. MAT1 is a serine protease found to colocalize with E-cadherin at the intercellular apical junctional complexes (AJC)[21]. MAT1 knockdowns have impaired ability to develop an

appropriate TER and were also shown to have 3.5- to 4-fold increased levels of CLD2 at their tight junctions. However, the barrier defect was alleviated when cells were also depleted of CLD2[21] as enhanced TER development was observed [21]. The rescue of TER supports the notion that MAT1 plays a role in barrier integrity via CLD2. This mechanism will be further investigated in the TC45 dominant negative cell line to evaluate if an increase of claudin-2 by matriptase-1 is TC45 dependent.

As genome-wide-association-studies (GWAS) indicated, PTPN2 dysfunction has been linked to IBD susceptibility [11]. Our studies will aid in elucidating the pathogenesis of IBD ultimately providing insight for potential therapeutic development.

II. MATERIALS AND METHODS

Materials pEGFP-C1-TC45 (provided by Tiganis Lab, Monash University, Australia), pCMV-HA construct and Lenti-X Tet-On Advanced Vector Set (Clontech, Mountain View, CA), Doxycycline (Sigma, St. Louis, MO), Human recombinant IFN-γ (Roche, Mannheim, Germany), monoclonal mouse anti-PTPN2 antibody CF-4, which detects the 45-kilodalton and the 48-kilodalton isoforms (Calbiochem, San Diego, CA), rabbit anti-CLD2 (Invitrogen, Carlsbad, CA), anti-phospho-STAT1 (Tyr^{701}), anti-STAT1, and monoclonal mouse anti-β-Actin (Sigma, St. Louis, Missouri) were obtained from the sources noted. Millicell culture plate inserts were purchased from Millipore Corporation (Millipore, Bedford, MA). All other reagents were of analytical grade and acquired commercially.

Overall Strategy EGFP-TC45 constructs were mutagenized to form both the C216S mutant and N206-fs. These constructs were subcloned into pCMV-HA vector in order to switch protein tags. PCR was used to add compatible restriction enzyme sites, Bam-HI and MluI, to the HA-TC45 constructs (wild-type, C216S and N206-fs). These inserts were subcloned into the lentiviral vector, pLVX-Tight-Puro. The lentiviral HA-TC45 constructs were transfected into a packaging cell line to produce lentiviruses for each construct. These lentiviruses transduced human colonic epithelial cell lines, HCA7, to produce a cell line that stably expresses dominant negative TC45. The dominant negative cell lines were then evaluated.

Subcloning and Propagation of Vectors in DH5α Constructs in pEGFP-C1 and pCMV-HA vectors were transformed into DH5α competent cells (Invitrogen, Carlsbad, CA). 50ng of DNA was added to 50µl of freshly thawed DH5α and left on ice to equilibrate for 30 minutes. The bacteria were then heat shocked at 45°C for 1-2 minutes and then placed back on ice for 5 minutes. 250µl of Super Optimal Broth with Carbolite repression (SOC) medium (Invitrogen, Carlsbad, CA) was added. The SOC diluted bacteria were transferred to a 15 ml falcon tube and placed in a 37°C shaker at 250 rpm for 60 minutes. The DH5α was then streaked on LB/agar plates with 30µg/mL of kanamycin (for pEGFP-C1 vectors) or carbenicillin (for pCMV-HA vectors). The plates were incubated at 37°C overnight. Colonies were selected and suspended in 4 ml of Luria Broth (1% tryptone, 1% NaCl, 0.5% yeast extract) containing the appropriate antibiotic (12µL kanamycin or 8µL carbenicillin) to propagate overnight. A Qiagen Mini Prep Kit (Qiagen, Valencia, CA) was used to isolate DNA from bacteria. The DNA was then assessed for purity and concentration by measuring the 260λ (sensing nucleotides), 280λ (sensing proteins) and 230λ (sensing organic compounds) absorbances using a Nanodrop. These absorbances were then calculated into ratios of 260/230 and 260/280 to assess how many nucleotides per contaminant were present. The 260λ absorbance was also used to calculate the concentration of DNA using Beer's Law ($A = \varepsilon l c$).

Restriction Digests of EGFP-TC45 and CMV-HA Backbone In order to subclone the TC45 construct into the CMV-HA vector, both vectors were digested. The EGFP-TC45 vectors, CMV-HA backbones were digested with two restriction digest enzymes, BglII and KpnI (New England BioLabs Inc., Ipswich, MA), both of which cut the vector

leaving “sticky ends”. This allowed for directional ligations of the inserts. After one-hour digestions, the products were run on a 0.8% agarose gel to evaluate the success of the digestion.

DNA Agarose Gel 0.8% agarose was dissolved into 1X TBE solution and 2µl of ethidium bromide was added. The solution was poured into a gel cassette and left to solidify. Purified DNA was suspended in loading dye (10mM Tris-HCL, pH 7.6, 0.03% bromophenol blue, 0.03% xylene cyanol FF, 60% glycerol and 60mM EDTA) and loaded into gel next to a GeneRuler 1kb Plus DNA Ladder (Invitrogen Corporation, Carlsbad, CA). Gels were visualized under a UV lamp.

DNA Gel Extraction, Concentrator and Quantification After the appropriate bands were observed (TC45 insert is 1.6kb and pEGFP-C1 backbone is 3.8 kb) under the UV lamp compared to the DNA kb ladder, the insert was excised from the gel with a razor blade. A Gel Extraction kit (Qiagen, Valencia, CA) was then used to isolate the DNA from the agarose. Due to the low concentration DNA suspended in a large volume, a PCR clean up and concentrator (Zymogen, Irvine, CA) was used to achieve optimal concentrations. Purity and concentration of DNA was again analyzed by nanodrop.

Alkaline Phosphatase, CIP and Ligation Reactions Digested backbones were treated with Alkaline Phosphatase, Calf Intestinal (CIP) (New England BioLabs Inc., Ipswich, MA) in order to remove the 5’ phosphate group from the DNA to prevent self-ligation and therefore reduce empty vector background in cloning. Backbones were again purified

with PCR clean up and concentrator kit (Zymogen, Irvine, CA) to eliminate enzymes and excess nucleotides as well as be able to switch buffers. With clean inserts and backbones, a 3:1 insert to backbone ratio ligation reaction was set up (per manufacturer's instructions) using T4 Ligase (Invitrogen, Carlsbad, CA). Ligation reactions were carried out following company protocol and left over night. Ligation products were again purified using a PCR clean up and concentrator kit (Zymogen, Irvine, CA) and then transformed into either DH5α or STBL2 as described previously in subcloning and propagation of vectors.

Site-Directed Mutagenesis to Correct Frameshift Transformer Site-Directed Mutagenesis Kit (Clontech, Mountain View, CA) was used to insert one nucleotide between the HA sequences and TC45 start codons for all pCMV-HA-TC45 vectors (wild-type, C216S, N206-fs). The Clontech protocol was followed and primers used are listed in Table 1.

Polymerase Chain Reaction to Introduce BamHI and MluI sites A BAM-HI restriction enzyme site was needed before the gene and an MluI site after in order to subclone the HA-TC45 sequences into lenti-x backbones. This was done using a high fidelity Phusion polymerase (Finnzymes, Keilaranta, Espoo, Findland) for a Polymerase Chain Reaction (PCR). The primers used are listed in Table 1. Four 50μL reactions were set up as directed by Finnzymes with modifications made to use of the GC buffer and increased DMSO to 3% of the reaction due to the nucleotide GC rich content.

Initial denaturation occurred at 98°C for 30 seconds. Cycling denaturation occurred at 98°C for 5-10 seconds. Annealing temperature was adjusted to 62.5°C for 30 seconds and extension occurred at 72°C for 15-30 seconds per base pair (108 seconds). Final extension was also set to 72°C but for 7 minutes. A sample of each reaction was run on a 0.8% agarose gel to confirm success by observing bands at 1.6kb, followed by a PCR clean up and concentrator kit (Zymogen, Irvine, CA) and nanodrop concentrator assessment.

Subcloning into Lentiviral Constructs PCR products of the HA-TC45 as well as lentiviral pLVX-Tight-Puro backbones were digested with MluI and BamHI-HF for one hour or 15 min, respectively. Digested products were cleaned up using a PCR clean up and concentrator kit (Zymogen, Irvine, CA).

Again, in order to improve ligation yield, backbones were treated with alkaline Phosphatase (New England BioLabs Inc., Ipswich, MA) to remove the 5' phosphate groups preventing self-ligation after restriction digests.

Ligations were carried out as specified above and confirmed by running a sample of the completed reaction on an agarose gel to observe a band at 9.6 kb. The rest of the sample was purified using a PCR clean up kit and quantified.

DH5α could not be used since they produced small colonies surrounded by satellite colonies indicating that the colonies were not healthy and they yielded very low amounts of DNA if any at all. Further research concluded that DH5α was an inappropriate host for replication of the Lenti-X vector due to the long terminal repeats (LTRs) that composed approximately 17% of the vector. Stbl2 E.coli was selected and

transformed with the Lenti-x-HA-TC45 vectors. Healthy colonies formed and appropriate concentrations of DNA were achieved (1-20μg/μl).) Due to the nature of the Lenti-X vectors that contain long terminal repeats (LTRs), the newly ligated constructs needed to be propagated in STBL2.

Lenti-X vectors, pLVX-Tet-On Advanced and pLVX-Tight-Puro, were transformed into STBL2 and STBL3 (Invitrogen, Carlsbad, CA) following company protocol. Mini and Maxi preps (Qiagen) were used to isolate the DNA. DNA was then sent to sequencing for verification that the Lenti-X vectors contained the HA-TC45 inserts and all were in the correct frame.

Cotransfection of Lenti-X 293T Packaging Cell Line for Lentiviral Production

Verified p-LVX constructs and Lenti-X HTX Packaging Mix (Clontech, Mountain View, CA) were cotransfected into Lenti-X 293T Packaging Cells (Clontech, Mountain View, CA) following company protocol with the aid of Polybrene Infection/Transfection Reagent (Millipore, Bedford, MA). Tet-On transactivator viruses were also produced in this manner.

Lentiviral Titers After two days the virus-infected media was harvested and concentrated. The viral titer was tested in two ways: first, using the Lenti-X GoStix (Clontech, Mountain View, CA) and secondly, with the Lenti-X p24 titer Kit (Clontech, Mountain View, CA). GoStix are designed to instantly confirm the presence of lentivirus in the packaging cell supernatant. The test detects p24, a viral protein present on the outside of the viral capsid and therefore measures total viral particles instead of viably

active, infectious particles. It is estimated that for most viral preparations the ratio of infectious units (IFU) to viral particles is 1:20 to 1:50. As reported by Clontech, a clear band generated on the stick indicates that there is 5 x 10^5 IFU/ml or greater in the cell supernatant. Clontech determined this concentration using flow cytometry of transduced HT-1080 cells (Clontech p24 Titer Kit Protocol). Supernatant was harvested from 293T packaging cells that contained Lenti-X-Teton, Lenti-X-HA-TC45, Lenti-X-HA-TC45^{C216S} and Lenti-X-HA-TC45$^{N206\text{-}fs}$ viruses separately and tested on the GoStix. Samples from all of the supernatants all generated a band on the GoStix indicating viruses were successfully being produced.

For a more accurate measurement of the individual viral titers, the Lenti-X p24 Rapid Titer Assay was used. This assay utilizes standard ELISA methods in which the wells of the microtiter plate are coated with anti-HIV-1 p24 capture antibody. Upon exposure to the dilutions of viral stocks, p24 binds the wells and then is detected in a typical "sandwich" ELISA format with a biotinylated anti-p24 secondary antibody, a streptavidin-HRP conjugate and a color producing substrate. Color intensity is then measured using a spectrophotometer and compared to a standard curve. The calculated titer results of the absorbance readings that fell within the range of the standard curve are summarized in Table 2.

Cell Culture The human colonic epithelial cell line, HCA7, was used for all experiments in this study. HCA7 cells display the functional properties of colonic crypt epithelial cells, and are capable of forming polarized monolayers with tight junctions. Cells were grown in DMEM media with 5% Tet approved newborn calf serum (Clontech Mountain

View, CA) in 75 cm^2 flasks. The cells were trypsinized and passaged at 95% confluency, and split 1:5.

For *in vitro* transepithelial electrical resistance (TER) experiments, HCA7 cells were seeded onto 12mm Millicell-HA culture plate inserts (filter membranes) and grown for 14 days before study, at which time they had stable values of transepithelial electrical resistance indicating that the cellular monolayers had established tight junctions. Doxycycline was used to activate the tet protein, thus inducing transcription of the HA-TC45 constructs. Doxycycline (15μM) and IFN-γ (200U/mL) was added basolaterally.

For confocal analysis, cells were seeded on 6-well Millicell-HA culture plates with glass-cover slides placed on the bottom. Cells were grown for 1 day prior to treatment with doxycycline.

Transient Transfections Approximately 2 x 10^6 parental HCA7 cells were electroporated with 25μg of DNA for each construct. Cells were seeded onto inserts and left to recover for 48 hours. 48 hours yielded maximum expression in HCA7s after transfection with an EGFP control. At 48 hours, inserts were then stimulated with IFN-γ for 6 hours before being lysed.

RNA Isolation and Real-Time Polymerase Chain Reaction Total RNA was isolated and DNA was removed from transduced-HCA7 cells using the Direct-zol RNA MiniPrep kit (Zymogen, Irvine, CA) according to manufacturer's instructions. RNA purity and concentration were assessed by absorbance at 260 and 280 nm. Complementary DNA

(cDNA) synthesis was performed to assess mRNA levels of tet protein using a High-Capacity cDNA Reverse Transcription Kit (Applied Biosystems, Foster City, CA). Quantitative Reverse-Transcriptase Polymerase Chain Reaction was performed using MESA GREEN qPCR MasterMix Plus for SYBR Assays (Eurogentec, San Diego, CA on a StepOnePlus Real-Time PCR system using Step One Software v2.0 (Applied Biosystems). Measurements were performed in triplicate, human GAPDH was used as an endogenous control, and results were analyzed by the ΔΔCT method (normalized to control and to housekeeping gene).

Preparation of Cytoplasmic Lysates On the day of the experiment, cells from inserts containing HCA7 monolayers were suspended in ice cold lysis buffer (50mM Tris, 150mM NaCl, 0.1% SDS, 0.5% sodium deoxycholate, 20μM NaF, 1mM EDTA, 1μg/ml antipain, 1μg/ml pepstatin, 1μg/ml leupeptin, 1mM $NaVO_3$, 100μg/ml phenylmethylsulfonyl fluoride), vortexed thoroughly, and subjected to lysis using a 0.22 gauge needle. The lysates were centrifuged at 10,000 rpm for 10 min to remove insoluble material, and an aliquot was removed from each sample to determine protein content (Bio-Rad protein assay according to manufacturer's instructions). Samples were resuspended in loading buffer (50mM Tris, pH 6.8, 2% SDS, 100 mM dithiothreitol, 0.2% bromophenol blue, 20% glycerol) and boiled for 5 min.

Western Blotting to Assess Protein Levels Samples suspended in loading buffer were loaded onto a 4-15% gradient polyacrylamide gel in order to resolve proteins. The proteins were transferred onto a polyvinylidene difluoride membrane (Millipore,

Billerica, MA). The membrane was incubated in blocking buffer (5% BSA in 0.1% TBST) for 1 hr followed by overnight incubation of the membrane in blocking buffer containing primary antibody diluted 1:1000. This was followed by three 5-min washes with 0.1% TBST. After washes, secondary antibody (goat-anti-rabbit, Cell Signalling, Danvers, MA, or goat-anti-mouse IgG conjugated to horse radish perodixase, BD Pharmigen, San Diego, CA) diluted 1:2000 was added to the membrane and incubated for 30 min. This was followed by three more 5-min washes with wash buffer. The membrane was then treated with chemiluminescent solution according to the manufacturer's directions (Thermo Scientific, Rockford, IL) and exposed to film. Densitometric analysis of the blot was performed using Image J software (NIH).

Transepithelial Electrical Resistance Transepithelial electrical resistance (TER) across HCA7 monolayers was assessed by voltohmeter (WPI, Sarasota, FL) and companion electrodes (Milipore, Bedford, MA). Measurements were calculated in $\Omega \cdot cm^2$. When evaluating DOX and IFN-γ co-stimulated conditions, TER was normalized to the TER at the time of DOX treatment and then averaged.

Cell Fixation and Immunocytochemical Staining Cells were seeded on glass cover slips in 6-well Millipore plates. Media was aspirated and replace with 1 ml of 4% paraformaldehyde (PF) for 10 minutes covered from light. 4% PF was aspirated and wells were washed 3 x 5 minutes with PBS. Cells were then permeabilized with 0.1% triton-X-100 solution, incubated for 10 minutes. Wells were again washed 3 x 5 minutes with PBS. After washes, cells were treated with 50mM of NH_4Cl for 5 minutes and washed

again, 3 x 5 minutes with PBS. Cells were blocked with 1% BSA in PBS for at least 15 minutes and left in 4°C until probed.

Slides were probed with 1:50 dilutions of primary antibodies (PTPN2, HA, MAT1 and CLD2 from sources listed above) for 2 hours to overnight. After incubation, slips were washed 3 x 5 minutes with PBS and then probed with a 1:100 dilution of secondary Alexafluor antibody for 1 hour. Slides were washed again with PBS for 3 x 5 minutes then stained with Hoechst solution to bind to the DNA for visualization of the nucleus, washed again and mounted onto slides.

Statistical Analysis All data are expressed as means ± SEM for a series of experiments. Statistical analysis was performed by Student's unpaired t-test or analysis of variance (ANOVA) and Student-Newman-Keuls post-test using Graph Pad Instat 3 software (Graph Pad Software, La Jolla, CA). P values < 0.05 were considered significant.

III. RESULTS

Development of CMV-HA-TC45 Constructs

The overall goal of our study was to identify the functional consequences of loss-of-function mutations in PTPN2 gene for IFN-γ signaling and epithelial barrier function. In order to achieve this, we generated two PTPN2 mutants. First, we generated an active-site mutation that alters the critical cysteine residue Cys216 to Ser216 ($TC45^{C216S}$), and secondly, we generated a frameshift mutation at Asp206, which models the single-nucleotide polymorphism (SNP) rs34387614 ($TC45^{N206\text{-}fs}$) (confirmed by sequencing seen in Figure 3). Both of these mutants were created using a TC45 construct fused to an EGFP tag that was generously provided to us by Dr. Tony Tiganis (Monash University) [23].

Transient transfections were then performed with these vectors to assess the effects of mutations. Unfortunately, the EGFP protein tag affected the trafficking pattern normally observed for the TC45 splice variant. At 45kDa, this variant is able to enter and exit the nucleus via the nuclear pore without an NLS signal. However, with the addition of the large EGFP protein, approximately 29kDa, TC45 can no longer pass through the pore and thus it accumulates within the nucleus as seen in Figure 4. Therefore, a new, more appropriate tag was required.

I therefore switched to a hemagglutinin (HA) tag because it is smaller (1.1KD) and therefore less likely to interfere with the protein's normal activity and trafficking pattern as seen with the EGFP tag. A dominant negative model of HA- $TC45^{C216S}$ was then developed in human colonic epithelial cell lines via lentiviral transduction in order to allow us to study the functional effects of mutations in TC45.

We initially set out to incorporate the C216S and the N206-fs mutations in a stable transfection cell line model. I first generated constructs that fused the TC45 sequence to a HA tag, thus removing the hindrance of the large EGFP tag. EGFP-TC45 constructs (EGFP-TC45^{WT}, EGFP-TC45^{C216S} and EGFP-TC45$^{N206\text{-}fs}$) were digested with restriction enzymes, BglII and KpnI, and run on an agarose gel. Bands were observed at 1.6 kb and 4.6 kb for the wild-type, active site mutant and frameshift mutant. The 1.6 kb TC45 inserts were excised from the gel and purified. The same restriction digestions were performed with the CMV-HA vector to create a backbone into which the purified inserts were ligated.

Initial research confirmed the compatibility of the EGFP and CMV-HA vectors. However, there were no HA-tagged proteins detected in HCA7 cells transiently transfected with the CMV-HA-TC45 vectors. Upon a second evaluation of the Open Reading Frame (ORF) of the ligation product in the CMV-HA, a single nucleotide frameshift was discovered to have occurred between the DNA encoding the HA tag and the start codon of the TC45 sequences (Figure 5). The result was the expression of the HA protein alone since the frameshift resulted in a premature stop codon early in the TC45 sequence. Therefore no tagged protein was detected in the western blots, as the expressed protein was likely small enough to run off the gel.

Mutagenesis was performed to shift the reading frame back to the correct frame. Completion of the mutagenesis was confirmed by sequencing and again, input into the ORF reader.

Ultimately, completion of the CMV-HA-TC45 vector was verified by western blot detection of the protein (Figure 6). Empty CMV-HA, CMV-HA-TC45, CMV-HA-

TC45^{C216S} and CMV-HA-TC45$^{N206\text{-}fs}$ were electroporated into HCA7 cells and probed for expression of the HA tag as well as for TC45 protein. HA expression was found at the appropriate molecular weight for the wild-type and the active site mutation (45kDa). Interestingly, the insertion mutation proved to be a truncated protein with the HA probe binding around 27kDa (Figure 6).

Although these transfections were useful in verifying the integrity of the CMV-TC45 vectors (wild-type and mutants), it was important to note the inconsistency of the transient transfections. As seen in Figure 6, HA was detected in only two of the replicates for the HA-TC45$^{N206\text{-}fs}$ and wild-type. However, the tag appears in the HA-TC45^{C216S} for most replicates but to differing degrees.

Transient Transfections of CMV-HA-TC45 constructs

Despite the inconsistency of the transfections, these samples were further probed to evaluate the phosphorylation, and thus activation, of the TC45 substrate, STAT1 (Figure 7). All IFN-γ treated conditions showed the expected increase in phosphorylated STAT1 (pSTAT1) compared to total STAT1 in the lysates. While the HA-WT and the empty-CMV transfection control showed similar levels of pSTAT1 to untransfected cells after treatment with IFN-γ, both HA-TC45 mutants showed nearly a 2-fold increase in pSTAT1 compared to the control. Significance, however, was only achieved in C216S compared to wild-type control. The increase in phosphorylated STAT1 in the C216S treated condition indicates that TC45 activity was impaired due to this mutation, thus leaving the IFN-γ stimulatory pathway without normal regulation.

Development of Lenti-X-HA-TC45 Constructs and Lentiviral Production

In order to further investigate this effect of the C216S mutant, a more stable and consistent model was needed. Therefore, the HA-TC45 constructs were used to develop a lentiviral system. The lentiviral system is Tet-On inducible, which allows controlled expression of the dominant negative TC45 model in the cell lines. HCA7 cells were transduced with Tet-On transactivator lentiviruses using a ubiquitous promoter to express Tet-On proteins. The transgenic Tet cell lines were then transduced a second time with TC45 wild-type or mutant lentiviruses. These TC45 genes are under a Tet-On promoter that will only express the gene when cells are treated with doxycycline, a tetracycline derivative. When doxycycline binds the Tet protein that is being produced in the cell it causes a conformational change. The new conformation loses affinity for the inhibitory molecules that were bound and the Tet protein becomes active to induce transcription of the desired HA-TC45 proteins.

Subcloning the HA tagged-gene of interests out of the CMV vector and into the Lenti-X viral vector required a Polymerase Chain Reaction (PCR) to insert a BAM-HI restriction enzyme site before the gene and an MluI site after. With the appropriate restriction enzyme sites in place, the inserts and the pLVX-Tight-Puro (Lenti-X) backbones were digested and ligated overnight. Initially, DH5α was transformed using the ligation products to propagate the vector. However, the only colonies that grew on the LB plates were small and surrounded by satellite colonies, indicating that the colonies were not healthy. The subsequent mini- and maxi- prep's yielded very low amounts of DNA if any at all. Further research concluded that DH5α was an inappropriate host for replication of the Lenti-X vector due to the long terminal repeats (LTRs) that made up a

fair portion of the vector. A new strain of E. coli was needed to prevent the recombination between the LTRs that was occurring in DH5α. Stbl2 E.coli was selected because it is characterized to prevent LTR recombination with a slower metabolism. The STBL2 bacteria were transformed with the Lenti-x-HA-TC45 vectors. Healthy colonies formed and appropriate concentrations of DNA were achieved (1-20μg/μl).

The newly made Lenti-X-HA-TC45 constructs were co-transfected into a specialized human cell line, Lenti-X 293T, along with five other vectors that encode the viral packaging. The cells produce the viruses and then exocytose them into the media. Because the lentiviral system that was selected is Tet-On inducible, a Tet transactivator lentivirus was needed as well and was made using the same protocol totaling four viruses.

After two days the 293T viral infected media was harvested and concentrated. The viral titer was tested in two ways: first, using the Lenti-X GoStix and secondly, with the Lenti-X p24 titer Kit. Samples from all of the supernatants generated a band on the GoStix indicating viruses were successfully being produced. For a more accurate measurement of the individual viral titers, the ELISA Lenti-X p24 Rapid Titer Assay was used. The ELISA designated all samples to have a viral titer of 10^8 or higher. Specific values are summarized in Table 2.

Production of Tet-On and TC45 Dominant-Negative Cell Lines

Finally, to produce the stable cell lines, HCA7 cells were transduced with the newly synthesized lentiviruses. HCA7 cells were transfected with Tet-On lentiviruses at a multiplicity of infection (MOI) of 5 and then selected for with G418 antibiotic. The colonies that formed were isolated and expanded.

In order to select an optimal cell line, one that will produce maximal Tet-On protein, real-time polymerase chain reaction (RTPCR) was used to assess and compare the levels of transcription of the Tet-On gene by quantifying the Tet-On mRNA. As seen in Figure 8, transgenic cell line 13 generated 2-fold more Tet-On mRNA than the majority of cell lines. This line was selected for additional expansion and subsequent transduction with the TC45 mutant or wild-type lentiviruses.

The selected Tet-On cell line was further transduced by the TC45 lentiviruses and again selected with antibiotic, this time with puromycin. Colonies were isolated and expanded. The cells were then lysed and probed for HA to evaluate the success of the transduction by verifying the HA-TC45 proteins were being expressed. However, no HA tag was observed.

The lack of expression was attributed to using a low MOI. Tiscornia et al. discussed how to achieve much higher titers by incubating with cell supernatant for longer periods and then using gradient centrifugation[24]. Because ultracentrifugation was unavailable to our lab, the viruses were sent to core facilities at UCSD. However, production of the insertion virus was still attempted in lab.

Appropriate titer levels were achieved (specified in Table 3) allowing transduction with high MOIs of 50, 100 and 200. The process was repeated using these MOIs. Unfortunately, because of the high MOI used, individual colonies could not be isolated after each antibiotic selection.

The cells were screened for protein expression by western blot. First, they were probed for expression of transactivator protein (Figure 9). An increase in Tet protein was observed as the MOI increased from 50 to 100 as expected. Further, the cells were probed

for the HA tag in which a clear band was detected at the appropriate 45 kD molecular weight in the C216S mutant cell line (Figure 10). This indicates that the C216S mutant TC45 is indeed attached to a HA tag. Corresponding HA tags were not observed in the wild-type or N206-fs mutant. Additionally, the selected C216S cell line was probed for PTPN2 protein levels compared to control transactivator-expressing cells. A 1.5-fold increase of PTPN2 was observed in the dominant-negative cell line in contrast to control transactivator-alone expressing cells (Figure 11). As expected, an increase in PTPN2 protein was observed in the cell line that was transduced with a higher MOI of transactivator virus. This enables a higher expression of the tet transactivator protein which in turn increases transcription of the transgene, HA-TC45^{C216S}.

Co-localization of PTPN2 and HA was additionally verified using confocal microscopy. Figure 12 shows the appearance of HA in C216S above background control as well as the increase in PTPN2 in the dominant negative cell line. HA-PTPN2 appears to co-localize at the tight-junctions (indicated by the arrow head) as well as within the nucleus (indicated with arrows).

Because of the nature of lentiviral transduction where insertion of genes occurs at random it was necessary to confirm that insertion of transgenes did not disrupt critical housekeeping genes. Therefore, further evaluation ensured that the transduced cells maintained normal phenotypes, such as tight junction formation, that could have been disrupted with insertion of the lentiviral genes. The cell lines were evaluated without inducing the system with doxycycline to distinguish any differences that could be attributed to expression of the mutations. Transepithelial electrical resistance (TER) measurements were monitored to confirm phenotypic tight junction barrier resistance in

the transgenic cell lines. HCA7 cells achieve upwards of 600 $\Omega \cdot cm^2$ TER as reported by Lee et al [25]. As seen in Figure 13, all cell lines surpassed this TER threshold at 8 days this confirming the transduced cells have normal phenotypes.

C216S Mutant Enhances IFN-γ Signaling

To demonstrate a decrease in TC45 function in mutant cell lines, phosphorylation of TC45 substrates was quantified. The previous experiment investigating levels of pSTAT performed with transient transfections of the HA-TC45 constructs was repeated using the stable dominant negative cell lines. However, conditions required pre-treatment with doxycycline 48 hours to activate transcription of the C216S mutant prior to stimulation with IFN-γ for 6-hours. As with the transient transfections of the C216S mutant, a significant increase in pSTAT1 compared to total STAT1 was observed in C216S co-stimulated with doxycycline and IFN-γ when compared to control under the same conditions (Figure 14). Both C216S and control showed similar pSTAT1 responses to the IFN-γ stimulation alone. Interestingly, when compared to IFN-γ alone the control showed a dramatic decrease in pSTAT1 levels if treated with doxycycline prior to IFN-γ stimulation. However, expression of C216S PTPN2 appears to ameliorate this dampening effect by the doxycycline, surpassing the IFN-γ alone in C216S conditions, indicating C216S mutants do not provide typical PTPN2 downregulation of IFN-γ downstream signaling.

To ensure that the immunomodulatory effect of doxycycline in IFN-γ signaling was not an artifact of the transduced cells, the experiment was repeated using the transactivator cell line and parental HCA7 cells. Similar results were observed

demonstrating a decrease in phosphorylated STAT1 under doxycycline plus IFN-γ co-stimulated conditions compared to IFN-γ alone (Figure 15). This further supported the use of the transactivator cell line as the proper control.

Claudin-2 Mediated Decrease in Epithelial Barrier Integrity

Our group previously showed that in cells deficient in TCPTP expression following PTPN2 siRNA transfection, IFN-γ can induce expression of the pore-forming tight junction protein, claudin-2. To assess if C216S cells mimic the effect of PTPN2 siRNA, the expression and localization of claudin-2 in IFN-γ treated C216S cells was evaluated. C216S and control cells were grown on glass cover slips and treated with doxycycline for 48 hours followed by a 6-hour incubation with IFN-γ. The slides were then processed and probed for CLD2.

An overall increase in claudin-2 was observed in the C216S IFN-γ treated cells compared to control (Figure 16). The increase of CLD2 at the tight junctions provides an explanation for the increased permeability to electrolytes across the epithelial barrier. The increase in CLD2 seen at the tight junctions of the C216S cells should lead to augmented cation permeability across the cellular monolayer. The increase in ions permitted across the barrier draws water into the lumen, leading to the symptomatic diarrhea in IBD.

PTPN2 Accumulation at Tight Junctions in C216S Mutants

To investigate if the C216S mutant had an effect on TC45 trafficking patterns, the dominant negative cell line was analyzed via confocal microscopy following IFN-γ stimulation. As seen in Figure 12, prior to stimulation PTPN2 localizes throughout the

cell including the nucleus. However, specific to the C216S cells, small amounts of PTPN2 are seen localizing at the tight junctions. In order to observe the trafficking of PTPN2 in C216S cells in response to IFN-γ stimulation, C216S and control cells were again treated with doxycycline 48 hours prior to 6-hour stimulation with IFN-γ.

A dramatic increase in the amount of PTPN2 at the tight junctions was observed in the C216S dominant negative cells (Figure 17). While there was an increase of PTPN2 overall due to the induction of the transgene expression, localization to the tight junctions appears to be a unique feature of the C216S dominant negative cells.

Reduced Matriptase Facilitates Increased Claudin-2 in C216S Mutants

It has been found that rapid turnover of claudin-2 at the tight junctions is mediated by a specific protease, matriptase-1 (MAT1)[21].To determine whether MAT1 regulation of CLD2 requires TC45 activity, C216S dominant negative cell lysates were assessed to quantify the expression level of both of these proteins. Short-term increases in accumulation of claudin-2 at the tight junctions of C216S cells led to the investigation of MAT1 levels via western blot after 6- hour IFN-γ stimulation.

As seen in Figure 18, C216S shows a simultaneous decrease in MAT1 with an increase in CLD2 compared to control. This synchronized effect in the C216S dominant-negative model demonstrates MAT1 modulation of CLD2 likely occurs in a PTPN2-dependent manner.

Extended IFN-γ Stimulation Leads to a Decrease in Barrier Resistance

To investigate if the C216S mutation ultimately results in greater barrier permeability in response to IFN-γ treatment, dominant negative cell lines were grown on inserts and monitored using TER measurements. Both C216S and control cells were treated with doxycycline for 48 hours before stimulation with IFN-γ for 72 hours. However, this protocol did not permit a change in media for 5 days. The effect of serum starvation was clear in the TER measurements after this duration of time and no significant difference between conditions could be discerned (Figure 19).

In the interest of decreasing the amount of time the cells would be incubated without new media, the incubation with doxycycline was decreased from 48 hours to 24 hours before stimulation with IFN-γ. Also, in the interest of time, the concentration of IFN-γ employed was increased from 200 units to 1,000 units per milliliter in order to elicit a stronger response in less time as used previously [3].

Both control and C216S mutant cells show large increases in TER (664 and 514 $\Omega \cdot cm^2$) further supporting that DOX has immunomodulatory effects (Figure 20). However, C216S expressing cells show a reduced TER compared to control after IFN-γ stimulation. At 6 hrs, C216S expressing cells have on average a 150 $\Omega \cdot cm^2$ difference lower than control. This difference was further enhanced to 216 $\Omega \cdot cm^2$ at 12-hour post IFN-γ treatment. This represents a compromised barrier in C216S expressing cells compared to control, indicating that C216S mutants decrease the protective ability of TC45 to maintain barrier integrity.

IV. DISCUSSION

PTPN2 has previously been linked to Crohn's disease where it has been demonstrated to have an important role in regulating the signaling pathway of the pro-inflammatory cytokine, IFN-γ[26]. Additionally, SNPs in the PTPN2 locus found by Genome-Wide Association Studies (GWAS) to be associated with CD patients could lead to loss-of-function mutations[11]. This study explored the biological consequences that accompany loss-of-function mutations in the TC45 isoform of the PTPN2 protein product, TCPTP, that include exaggerated IFN-γ signaling which could contribute to the development and progression of Crohn's disease.

My experiments required a stable model to further evaluate the disruptions in PTPN2 function when mutations occur within the active site of the TC45 phosphatase such as the C216S mutation. It was confirmed that a new model was necessary when the HA-TC45 constructs were transiently transfected into the HCA7 cells and expression of all three constructs was never achieved within a single trial (Figure 6). However, despite the issues with expression of the wild-type and frameshift mutations, significance was still established with the active site mutation when evaluating levels of phosphorylated STAT1. This encouraged further study yet it was obvious a new model was needed.

To develop a stable model, a lentiviral system was chosen. It was first necessary to generate the constructs fused to an appropriate tag incorporated into a lentiviral vector. When producing the virus, a few discrepancies arose particularly in titering and identifying ideal MOI. Although Core facilities produced titers similar to those achieved with the p24 ELISA Titer kit, it is likely that the p24 kit provided titers much higher than the actual amount of live virus within those samples. This is due to the fact that 1:50

viruses produced from the packaging cells actually contain the necessary DNA for a live virus while the others are empty capsids. These empty capsids still express p24 proteins outside and therefore the ELISA kit has no ability to distinguish between the live and empty viruses. The Core facilities, however, were able produce titers by colony forming units (CFUs) that will only account for live viruses therefore making their viral aliquots more potent with live viruses.

When using an MOI of 5, tet mRNA was detected in high amounts showing an increase of 10 fold for colony 13 compared to other transduced cells. However, these colonies did not show high enough expression of tet at the protein level to be detected in western blot or to induce transcription of the TC45 transgene when the cells were transduced with a TC45 lentivirus. Appropriate TC45 protein expression was finally achieved using the higher MOI of 100. In fact, the increase in MOI of the transactivator gene proved to be crucial in producing protein expression of C216S high enough for a dominant negative effect showing a 2.58-fold increase in total TC45 protein (Figure 11). Conversely, the use of high MOI increases the chances of adverse effects from the insertion of genes within the human genome. A higher MOI leads to increased insertion, which increases the possibility of these insertions occurring within critical genes and thus changing the phenotype of these cells. This is why these cells were further examined to ensure they maintained their colonic epithelial phenotype. This was verified by formation of a polarized monolayer as determined by TER measurements in Figure 13.

Once the C216S cell line was confirmed to produce the HA-TC45^{C216S}, my experiments first established the effect of the C216S mutant on regulation of phosphorylated STAT1. This was confirmed to be significant compared to the control tet

cell line co-stimulated with doxycycline (DOX) and IFN-γ. While DOX was used to turn on expression of the mutant TC45, throughout the course of this study DOX appeared to have a secondary effect demonstrating strong immunomodulatory properties. A dramatic 3-fold decrease in phosphorylated STAT1 of control DOX and IFN-γ conditions occurred compared to control treated with IFN-γ alone (Figure 14). This difference, that was consistently observed within the control conditions, led us to investigate this effect in the HCA7 parental cell line that had not been transduced. The same response to DOX was seen, confirming the immunomodulatory effect that DOX had on the pSTAT1 readout (Figure 15). This verified the co-stimulated control conditions as the proper comparison for examining the experimental C216S co-stimulated conditions. Using this control takes into account the DOX immunomodulatory properties and allows the effect of the TC45 mutant alone on IFN-γ signaling pathways to be evaluated. The effects of DOX in this system are independently of interest and deserve further study, and also sound a cautionary note for other investigators using similar systems.

To further assess the consequence of this active site mutation on TC45 function the cells were co-stimulated with DOX and IFN-γ, probed for PTPN2 and HA and then visualized via confocal microscopy. It was found that while PTPN2 was increased overall in the C216S cells, HA was prominent at the tight junctions following IFN-γ stimulation indicating that the $TC45^{C216S}$ mutants expressing the HA tag localized there as well (Figure 16). This occurred only in response to IFN-γ treatment suggesting that the membrane localization was in response to IFN-γ and not due to a non-specific mislocalization in transduced cells. This diversion in trafficking was a novel finding whose mechanism is unexplained by current literature and could be a direction for future

studies. A possible explanation may be that the amino acid change in the active site created higher affinity for different substrates that would attract TC45 to the cell membrane.

In order to elucidate how mutations in PTPN2 could lead to increased permeability in the epithelial barrier, I investigated the appearance of the pore-forming protein, claudin-2 (CLD2) in C216S cells co-stimulated with DOX and IFN-γ. It was observed that CLD2 localization at the tight junctions is increased while the diffuse, cytoplasmic CLD2 seen in the control appears to decrease (Figure 17). These findings support data from previous studies correlating loss of TCPTP with increased CLD2 [3].

Together, these data indicate that the pore-forming pathway triggered by IFN-γ signaling is not being properly regulated, leading to increased CLD2 at the tight junctions thus enhancing permeability between neighboring cells. This is further supported by the increase in pSTAT1 observed at this time-point, which, when stimulated by IFN-γ and left unregulated, results in added activation of STAT transcription factors that are potentially capable of binding to and promoting transcription of CLD2 as seen in Figure 17.

Furthermore, to investigate other potential contributors to the increase in CLD2 at the tight junctions, the regulatory phosphatase, matriptase-1 was examined. As Buzza et al reported, matriptase-1 associates with the intercellular apical adhesion complexes at the tight junctions [21]. Loss of MAT1 results in increased CLD2 at the tight junctions similar to the phenotype that was observed in my experiments. Matriptase-1 has been implicated in rapid turnover of CLD2 at the tight junctions and effects observed in the levels or location of MAT1 in C216S cells would indicate TC45 involvement in this

mode of regulation as well. Indeed, as seen in Figure 17, MAT-1 localized to the tight junctions of the control cells whereas little to no protein was observed in the C216S cells. This was a clear indication that TC45 is involved in the upregulation of MAT1.

In order to quantify the changes seen in the confocal images, protein levels were quantified via western blot. The results mirrored what was seen for MAT1 levels of Figure 17, however, the significant increase in CLD2 was not as striking in the confocal figure. This is most likely due to the high protein density at the tight junctions in the C216S cells even though cytoplasmic CLD2 appears to have decreased. What is observed in the localization of the proteins, as well as the significant inverse in protein expression levels (Figure 18) supports the hypothesis that MAT1 regulates CLD2 in a PTPN2-dependent manner.

TER data was collected to investigate long-term effects of the C216S mutants on IFN-γ signaling. The first attempt used the same treatment protocol as the previous experiments (15 mg/ml of DOX 48 hours prior to 200U/ml IFN-γ stimulation). However, we wanted to monitor the TER for 48-72 hours post-IFN-γ treatment which, when combined with 48 hours of DOX treatment, meant the serum would remain unchanged for 5 days. The result was that all of the cells, both C216S and control, showed signs of serum starvation wherein after the first day of IFN-γ stimulation all of the TERs decreased drastically (Figure 19). This decrease in TER masked any effect to be observed even between the IFN-γ versus untreated which has been documented to have significant differences [27]. Because of this, alterations were made in the treating the inserts: first the cells were treated with DOX (15μ/ml) for only 24 hours prior to IFN-γ stimulation and second, the inserts were treated with 1000 U/ml of IFN-γ instead of 200U/ml. This TER

data showed decreased resistance in the mutant cell lines compared to control indicating an increase in barrier permeability (Figure 20). DOX had a very strong effect on the resistance of all of the DOX treated inserts increasing some by nearly 700 $\Omega \bullet cm^2$. This DOX effect, again, made it difficult to discern the effect that IFN-γ was having in C216S-expressing cells compared to control. However, the difference was most exaggerated in the 12-hour-post-treatment time-point where C216S-expressing cells failed to protect the integrity of the tight junction barrier seal with a TER 216 $\Omega \bullet cm^2$ lower than control. In Figure 20B, it was also interesting that C216S-expressing cells showed a much lower response to DOX treatment alone. The C216S mutants were being expressed and thus most likely interfering with the protective effect that DOX was initiating in DOX-treated controls. The effect of DOX, again, deserves further investigation.

These data show significant changes in the IFN-γ signaling pathway due to the C216S TC45 mutation, supporting a study performed previously in our lab demonstrating elevated levels of pSTAT1 and claudin-2 in PTPN2 knock downs. This is important in showing that mutational defects that could potentially arise from SNPs in the PTPN2 locus demonstrate diminished activity of PTPN2. In turn, this would lead to lack of protection for the epithelial barrier. Dysregulation by the TC45 mutant appears to manifest by two avenues. First, increased IFN-γ signaling leads to enhanced expression of CLD2 that will allow cations to pass through the paracellular pathway. Next, CLD2 turnover at the tight junctions is decreased secondary to reduced MAT1 at the membrane, permitting CLD2 to remain at the intercellular junction longer, thus also contributing to increased paracellular cation permeability. Lack of negative regulation by the mutant

TC45 in both of these pathways attributes to the increase in barrier permeability within intestinal epithelial cells.

This study shows PTPN2 has a direct link to barrier dysfunction, however, the CLD2 protein turnover pathway has yet to be fully elucidated. It will be important in future studies to elucidate the link between matriptase-1 and TC45 to provide further insight into loss of barrier integrity in IECs and ultimately, additional understanding into the pathogenesis of Crohn's disease.

V. FIGURES

Figure 1 | IFN-γ Signaling Regulated by PTPN2 in Intestinal Epithelial Cells

IFN-γ binds to a receptor tyrosine kinase causing dimerization and phosphorylation. A signaling protein kinase, JAK, is recruited and subsequently phosphorylates the IFN-γ receptor tails. This phosphorylation leads to STAT recruitment and phosphorylation. Phosphorylated STAT dimerizes, exposing a nuclear localization signal that allows translocation into the nucleus where it acts to activate transcription of target genes. PTPN2 is responsible for dephosphorylation of the JAK and STAT proteins in the cytoplasm as well as the STAT dimers within the nucleus, promoting nuclear export. This turns off STAT-induced transcription and subsequent increases in IEC barrier permeability.

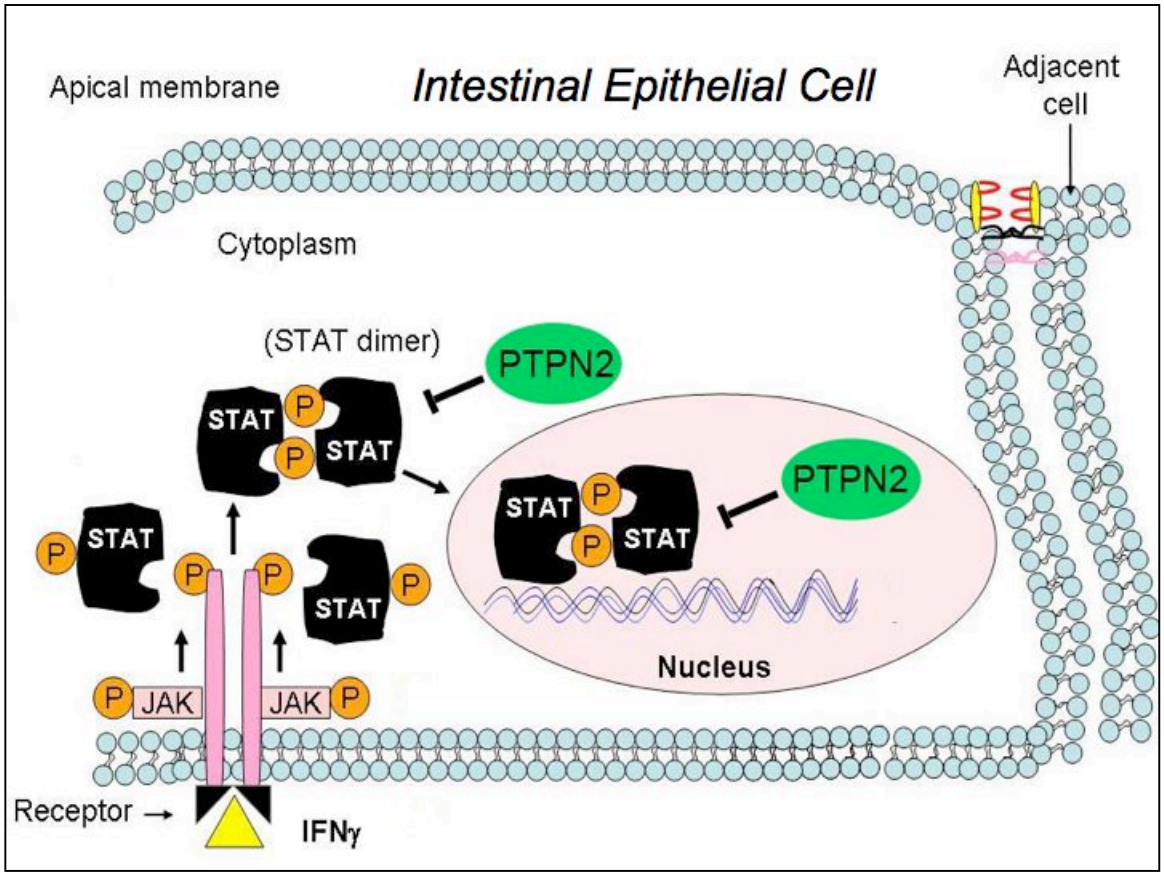
Apical membrane
Intestinal Epithelial Cell
Adjacent cell
Cytoplasm
(STAT dimer)
PTPN2
STAT
P
STAT
PTPN2
STAT
P
STAT
Nucleus
P
JAK
JAK
P
Receptor
IFNγ

Figure 2 | Ribbon Structure of PTPN2 with Residue Mutations

Panels A and B show the overall ribbon structure of TC45 with residues 216 cysteine and 206 arginine highlighted where the mutations take place. Panel A indicates the location of the active site where dephosphorylation occurs. Panel B is rotated to magnify the image seen in panel C.

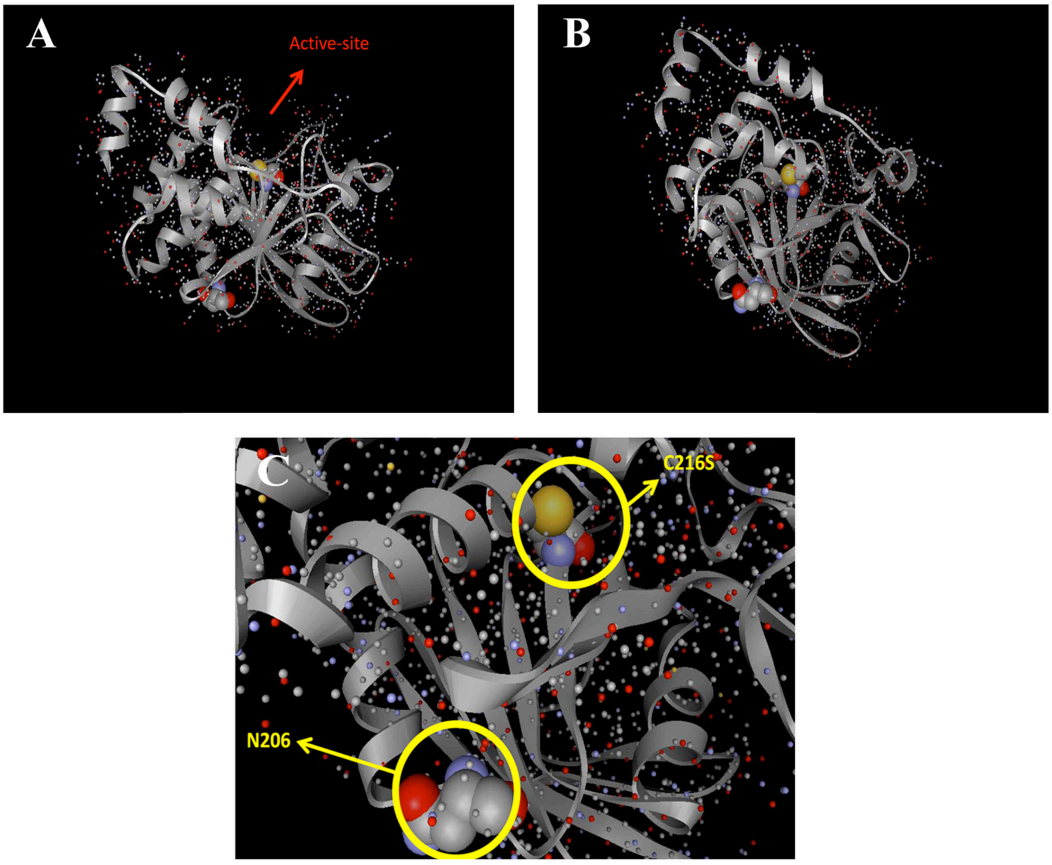
A
Active-site
B
C
C216S
N206

Figure 3 | Sequencing Confirmation of Mutagenesis in TC45 gene

Sanger sequencing confirmed the presence of both the C216S mutation and the N206 frameshift mutation.

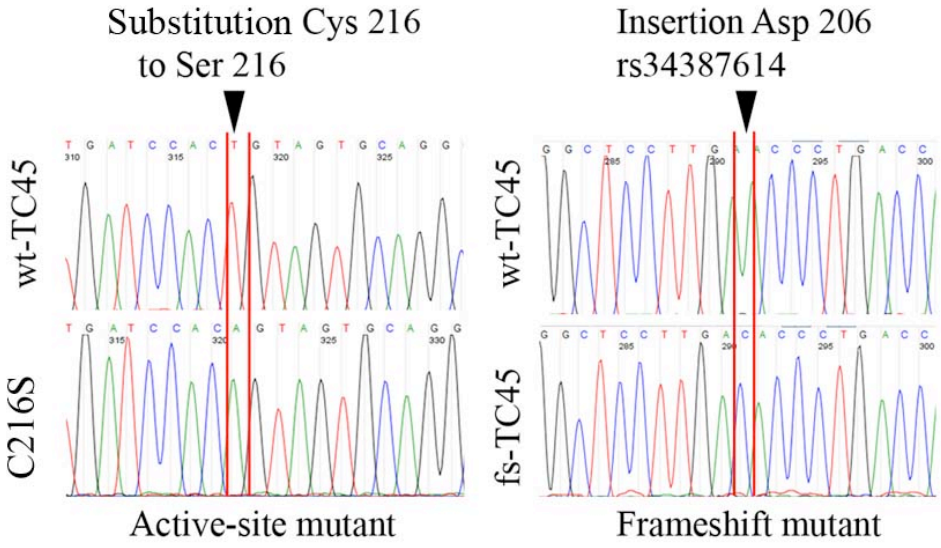
Substitution Cys 216
to Ser 216
Insertion Asp 206
rs34387614
wt-TC45
C216S
wt-TC45
fs-TC45
Active-site mutant
Frameshift mutant

Figure 4 | Disruption in Trafficking of EGFP-TC45

HCA7 cells were electroporated with EGFP-TC45 constructs. The left panel shows EGFP-TC45 fusion proteins sequestered within the nucleus after 96 hours post-transfection. The right panel shows the cellular monolayer was intact. A fluorescent microscope was used to capture the images. Arrows indicate single cell in monolayer with EGFP-TC45 within nucleus.

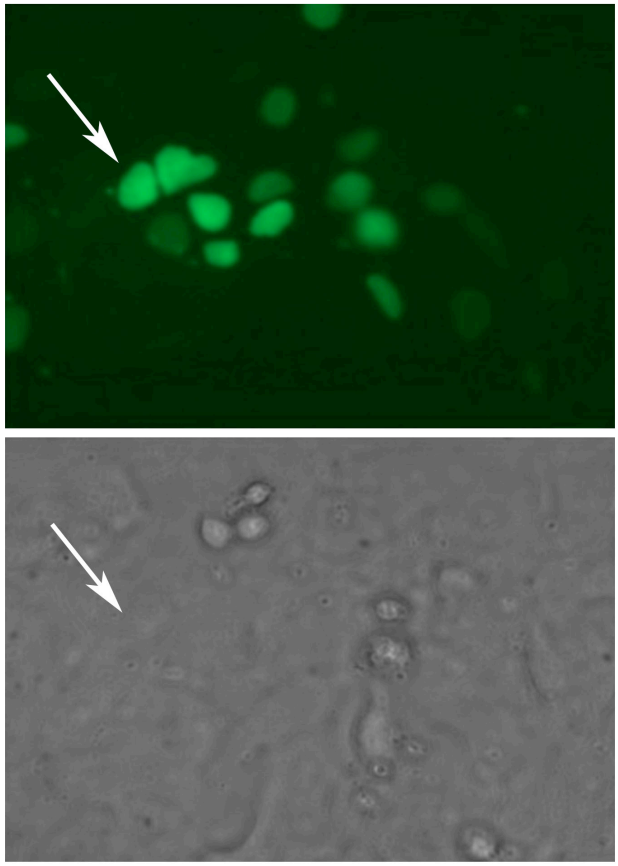

Figure 5 | Schematic of Construct Development

This is an overall illustration of the EGFP-TC45 constructs through the generation of the lentiviral vectors. A mutation occurred between the EFGP and CMV-HA subcloning constructs, indicated by the red arrow. Restriction enzyme sites for BamHI and MluI were then added by PCR and, finally, that insert was subcloned into the pLVX lentiviral construct.

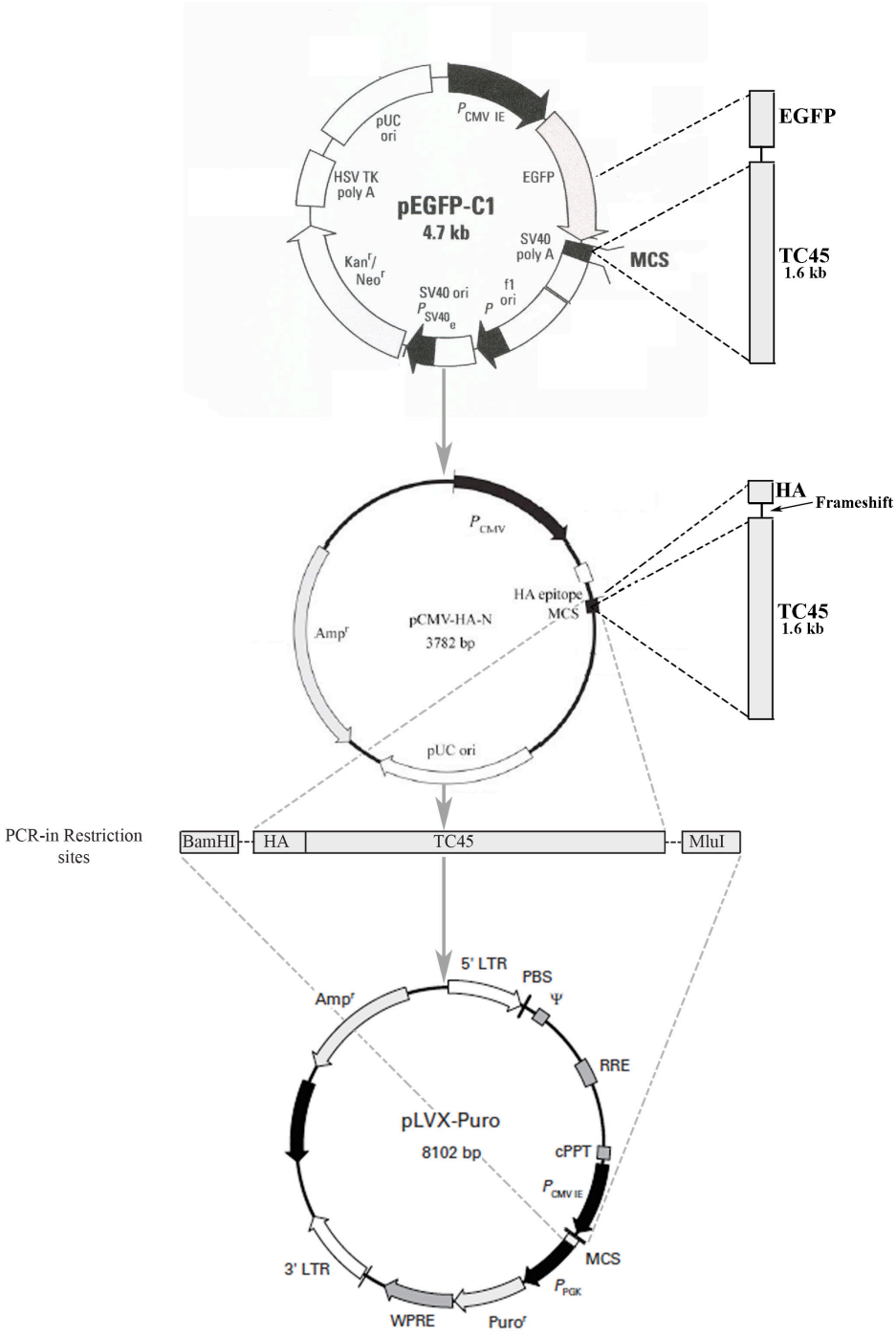
pEGFP-C1
4.7 kb
pUC ori
HSV TK poly A
Kan^r/ Neo^r
SV40 ori
f1 ori
EGFP
SV40 poly A
MCS
EGFP
TC45
1.6 kb
pCMV-HA-N
3782 bp
Amp^r
HA epitope
MCS
pUC ori
HA
Frameshift
TC45
1.6 kb
PCR-in Restriction sites
BamHI
HA
TC45
MluI
pLVX-Puro
8102 bp
Amp^r
5' LTR
PBS
RRE
cPPT
MCS
3' LTR
WPRE
Puro^r

Figure 6 | HA-TC45 Expression is Inconsistent in Transient Transfections

HCA7 cells were electroporated with the empty CMV-HA vector (control), CMV-HA-$TC45^{WT}$, CMV-HA-$TC45^{C216S}$ and CMV-HA-$TC45^{N206\text{-}fs}$ constructs to evaluate the validity of the constructs as well as assess any changes in activation of the TC45 substrate, phosphorylated STAT1. All four panels were probed for HA and showed differing results with only one or two of the constructs expressing but never all three. Both the wild-type and active-site mutant (C216S) have corresponding HA bands at 45 kD. The frameshift mutant (N206-fs) resulted in a premature stop codon to form a truncated protein with the HA band appearing at 27kD.

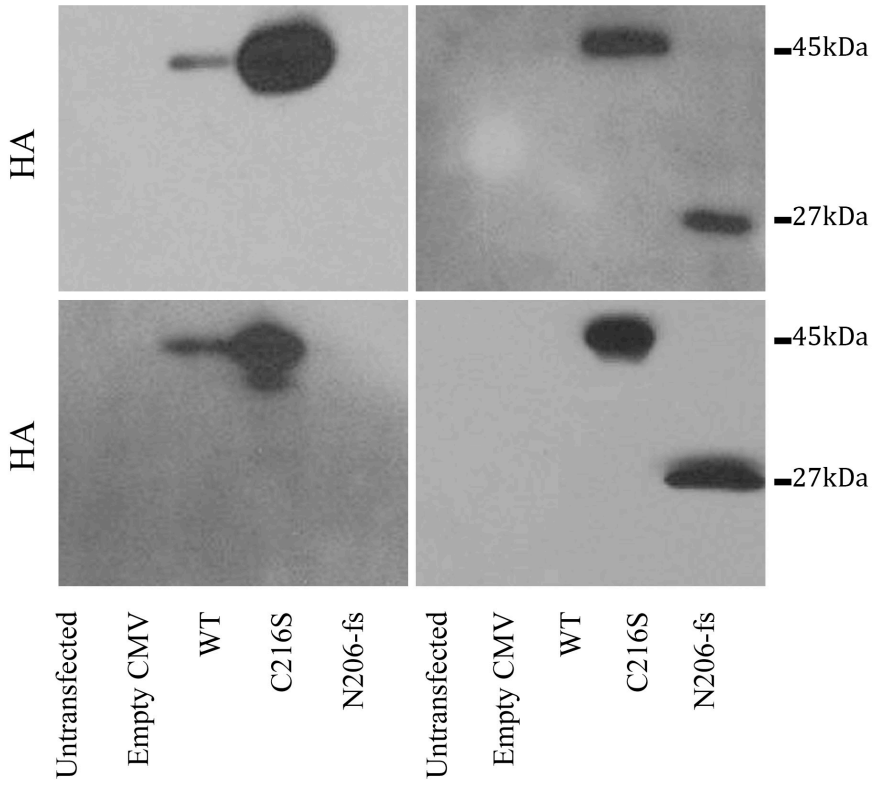
HA
HA
45kDa
27kDa
45kDa
27kDa
Untransfected
Empty CMV
WT
C216S
N206-fs
Untransfected
Empty CMV
WT
C216S
N206-fs

Figure 7 | The Effect of TC45^{C216S} on STAT1 Phosphorylation in Transient Transfections

IFN-γ (200 U/mL) induced STAT1 phosphorylation was quantified following 6 hours of treatment. IFN-γ-induced phosphorylation of STAT1 (pSTAT1) appeared in all treated conditions. However, conditions transfected with mutant constructs showed on average pSTAT1 levels that were nearly two-fold higher than in untransfected cells as shown by the histogram in the lower panel. Significance was achieved in treated C216S transfected conditions as compared to untransfected. β-Actin was used throughout as a loading control. The relative protein level was assessed by densitometry (n = 5). Data are expressed as an average ± SEM. (*$P < 0.05$ compared to IFN-γ-treated untransfected cells, using Anova and the Student-Newman-Keuls post-hoc test).

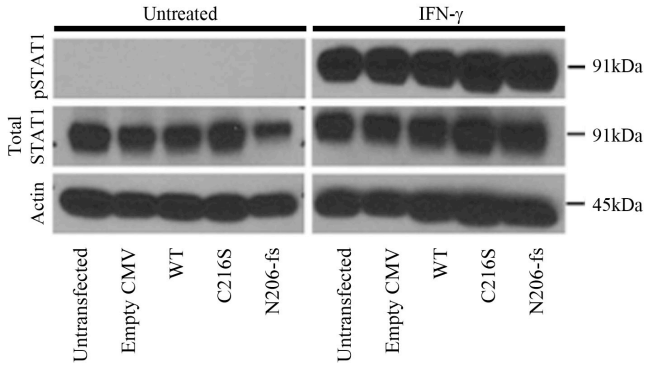
Untreated
IFN-γ
pSTAT1
Total STAT1
Actin
91kDa
91kDa
45kDa
Untransfected
Empty CMV
WT
C216S
N206-fs
Untransfected
Empty CMV
WT
C216S
N206-fs

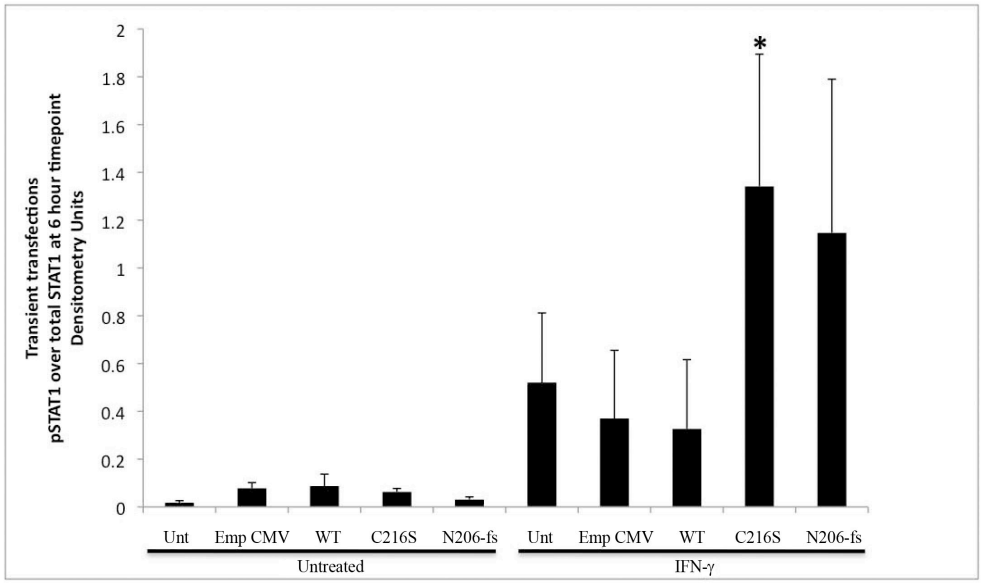
Transient transfections
pSTAT1 over total STAT1 at 6 hour timepoint
Densitometry Units
2
1.8
1.6
1.4
1.2
1
0.8
0.6
0.4
0.2
0
*
Unt
Emp CMV
WT
C216S
N206-fs
Unt
Emp CMV
WT
C216S
N206-fs
Untreated
IFN-γ

Figure 8 | Tet mRNA Quantification for Colony Selection

Tet mRNA levels in transduced cells were quantified for selection of a cell line with maximal Tet expression (n = 2). Colony 13 was calculated to have the highest concentration of Tet mRNA based on ΔΔCt analysis. Tet mRNA expression was normalized to the housekeeping gene GAPDH. Measurements were performed in duplicate.

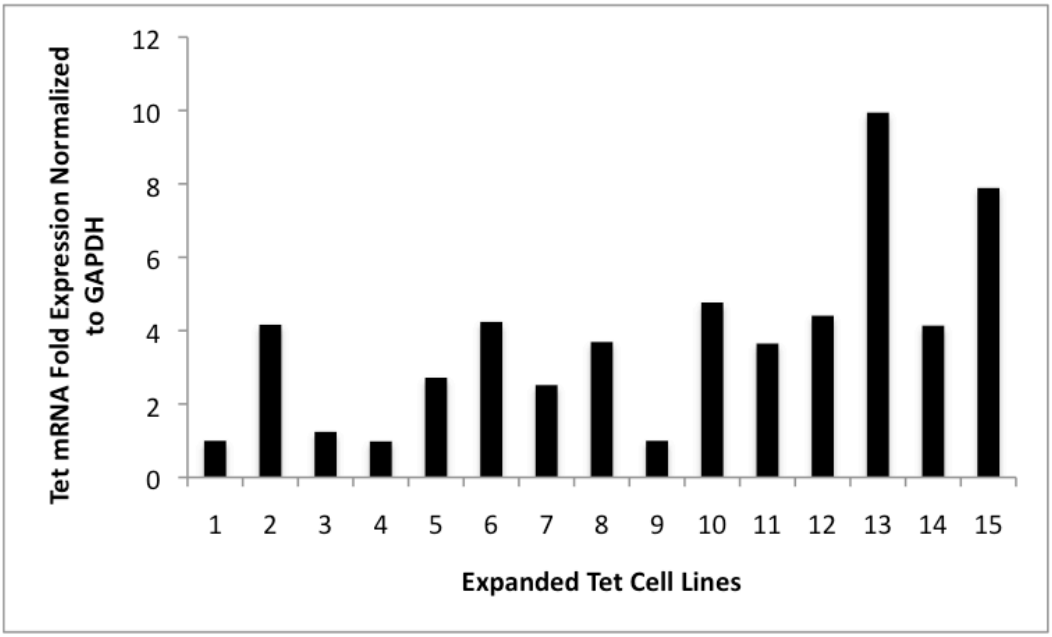
Tet mRNA Fold Expression Normalized to GAPDH
12
10
8
6
4
2
0
1
2
3
4
5
6
7
8
9
10
11
12
13
14
15
Expanded Tet Cell Lines

Figure 9 | Confirmation of Tet Protein Expression in Transduced HCA7 Cell Line

Tet protein expression was verified in cells transduced with a MOI of 50 or 100. An increase in Tet correlates with the increase in MOI with the tet lentivirus as expected. β-Actin was used throughout as a loading control.

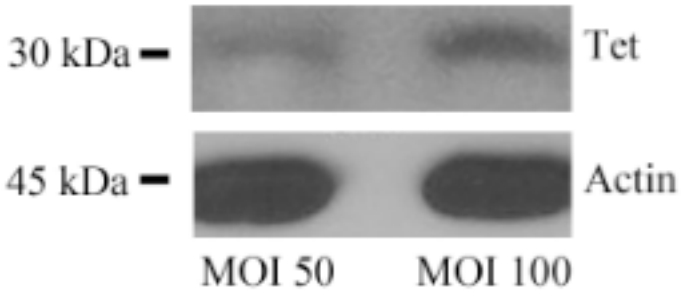
30 kDa
Tet
45 kDa
Actin
MOI 50
MOI 100

Figure 10 | Confirmation of HA-TC45^{C216S} Expression in Transduced HCA7 Cell Line

Transduced cells were treated with doxycycline (15 μg/ml) to induce transcription of HA-TC45^{C216S} (C216S). Lysate blots were probed with HA. HA was detected in the C216S dominant negative cell line. An increase in PTPN2 was seen in the doxycyline condition compared to untreated in the C216S cell line, which further indicated the TC45 construct was being expressed and adding to the total pool of PTPN2. β-Actin was used throughout as a loading control.

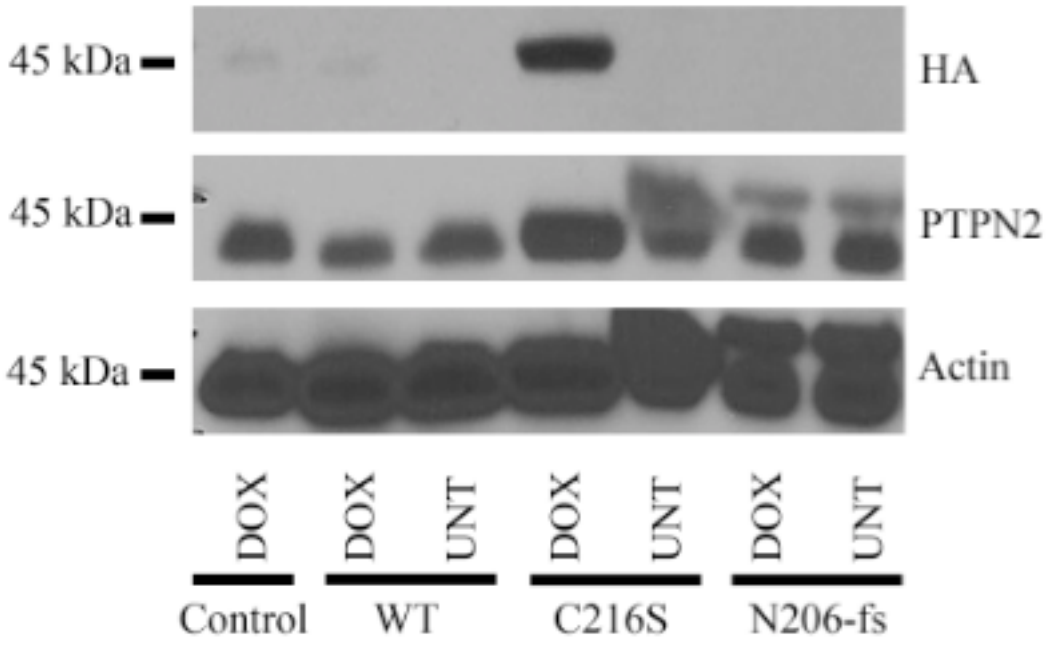
45 kDa
HA
45 kDa
PTPN2
45 kDa
Actin
DOX
DOX
UNT
DOX
UNT
DOX
UNT
Control
WT
C216S
N206-fs

Figure 11 | Increase in PTPN2 Expression in TC45^{C216S} Dominant Negative Cells

C216S dominant negative cells and tet expressing control cells were seeded on inserts and treated with doxycycline (15 μg/ml) 48 hours prior to the experiment. With an increase in transactivator tet protein expression that accompanies the higher MOI, PTPN2 protein increases. This is due to the added TC45^{C216S} expression induced by the extra transactivator protein available. β-Actin was used throughout as a loading control. Densitometry units refer to PTPN2 bands alone without normalization to actin.

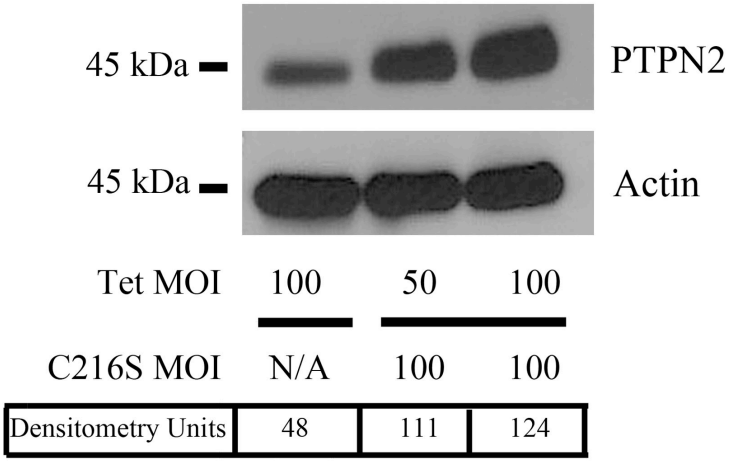
45 kDa
PTPN2
45 kDa
Actin
Tet MOI 100 50 100
C216S MOI N/A 100 100
Densitometry Units 48 111 124

Figure 12 | Colocalization Confirmation of PTPN2 and HA

C216S dominant negative cells and control tet expressing cells were seeded on glass slides and treated with doxycycline (15 μg/ml) to induce expression of the transgene, HA-C216S. Confocal imaging was used to assess colocalization of HA-PTPN2, verifying the integrity of the transgene protein as well as confirming an increase in mutated protein to ensure a dominant-negative effect. HA (red) had a 20% increase in the doxycycline-induced dominant negative cell line (DN HA-C216S). PTPN2 (green) also showed this appreciable increase in expression. Yellow indicates colocalization seen both within the nucleus (arrows) and at the tight junctions (arrow head). In the overlay, DAPI (blue) marks nuclear location and phalliodin (purple) outlines the cellular membrane actin.

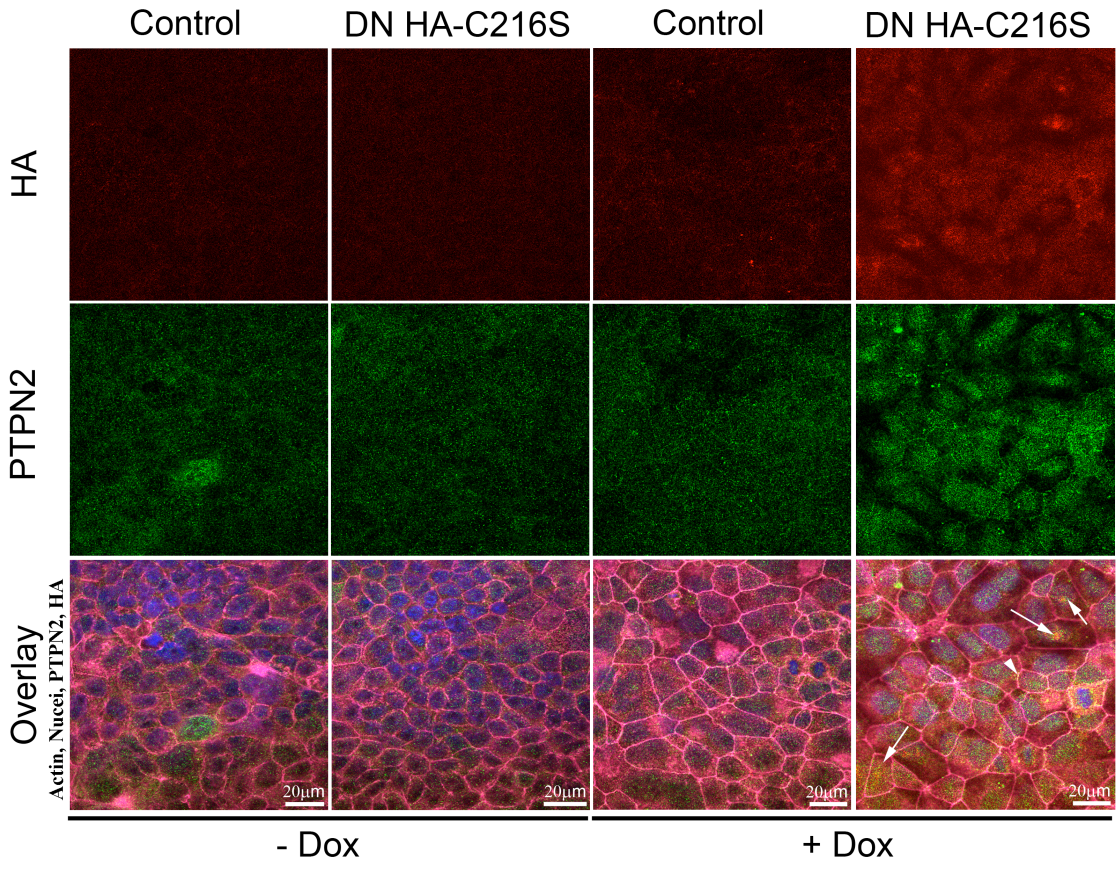
Control
DN HA-C216S
Control
DN HA-C216S
HA
PTPN2
Overlay
Actin, Nucei, PTPN2, HA
20μm
20μm
20μm
20μm
- Dox
+ Dox

Figure 13 | Confirmation of an Epithelial Resistance Phenotype in Transgenic Cells

$TC45^{C216S}$ (C216S) and tet expressing (control) cells were seeded ≈500,000 cells per 12 mm (0.6 cm^2 window area) insert. Transepithelial electrical resistance (TER) was monitored every other day. TER was normalized as $\Omega \cdot cm^2$. After one week of monitoring the cells had reached expected resistance levels indicative of the tight junction formation within the monolayer.

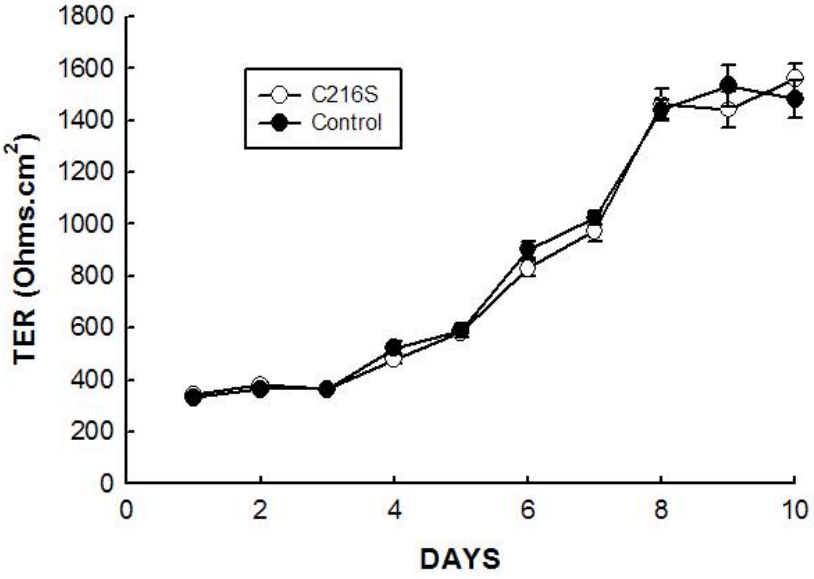
1800
1600
1400
1200
1000
800
600
400
200
0
TER (Ohms.cm^2)
C216S
Control
0
2
4
6
8
10
DAYS

Figure 14 | The Effect of Mutant TC45 on STAT1 Phosphorylation Following IFN-γ Stimulation

C216S and tet expressing control cells were seeded on inserts and treated with doxycycline (15 μg/ml) 48 hours prior to the experiment. IFN-γ (200 U/ml)-induced STAT1 phosphorylation was quantified following 6 hours of treatment. Characteristic IFN-γ pSTAT1 increase is seen in both C216S and control without dox induction of C216S expression. This pSTAT1 level was decreased in the co-stimulated dox and IFN-γ control condition indicating dox may have an immunomodulatory effect on this pathway and making this co-stimulated condition the proper control. When compared to the co-stimulated C216S mutant cells a significant increase in pSTAT1 is observed – with pSTAT1 levels enhanced by nearly 3-fold compared to control. β-Actin was used throughout as a loading control. The relative protein level was assessed by densitometry (n = 4). Data are expressed as a percentage of the control ± SEM (***$P < 0.001$ compared to untreated cells, using Anova and the Student-Newman-Keuhls post-hoc test).

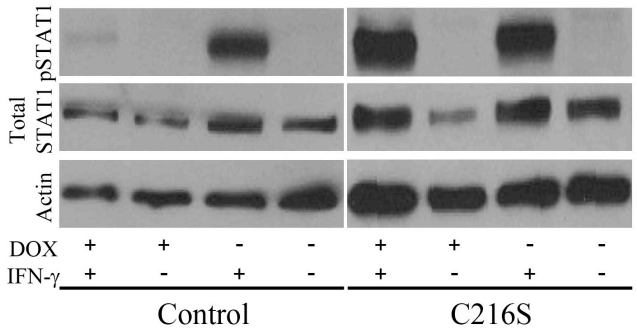
pSTAT1
Total STAT1
Actin
DOX + + - - + + - -
IFN-γ + - + - + - + -
Control
C216S

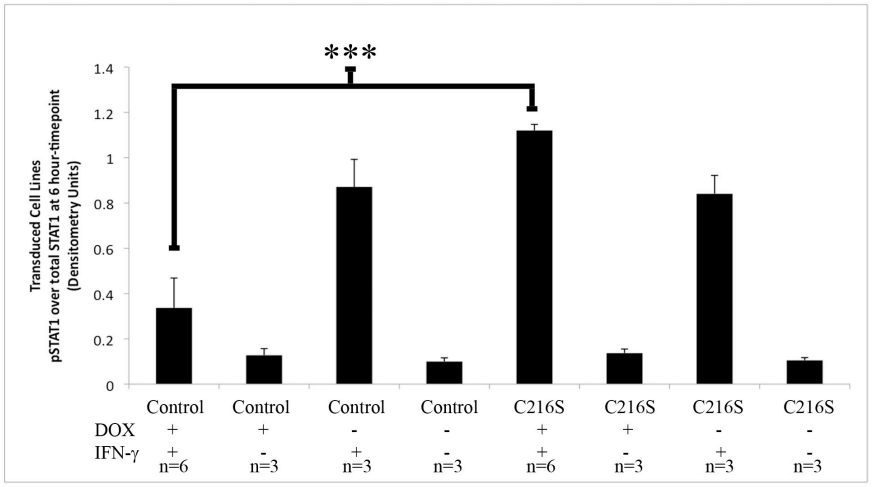
***
Transduced Cell Lines
pSTAT1 over total STAT1 at 6 hour-timepoint
(Densitometry Units)
1.4
1.2
1
0.8
0.6
0.4
0.2
0
Control Control Control Control C216S C216S C216S C216S
DOX + + - - + + - -
IFN-γ + - + - + - + -
n=6 n=3 n=3 n=3 n=6 n=3 n=3 n=3

Figure 15 | The Effect of Doxycycline on IFN-γ Signaling in Parental HCA7 and Transgenic HCA7 Cells

Parental HCA7 and tet transduced HCA7 cells were seeded on inserts and treated with doxycycline (15 μg/ml) 48 hours prior to IFN-γ stimulation. IFN-γ (200 U/mL)-induced STAT1 phosphorylation was quantified after 6 hours of treatment. IFN-γ treatment alone showed high levels of pSTAT1 compared to total. This outcome was markedly reduced in the dox and IFN-γ co-stimulatory conditions mirroring the effect seen in Figure 14 with C216S mutant cells and tet transduced control cells. This implies that the effect of doxycycline is not an artifact of lentiviral transduction. β-Actin was used throughout as a loading control.

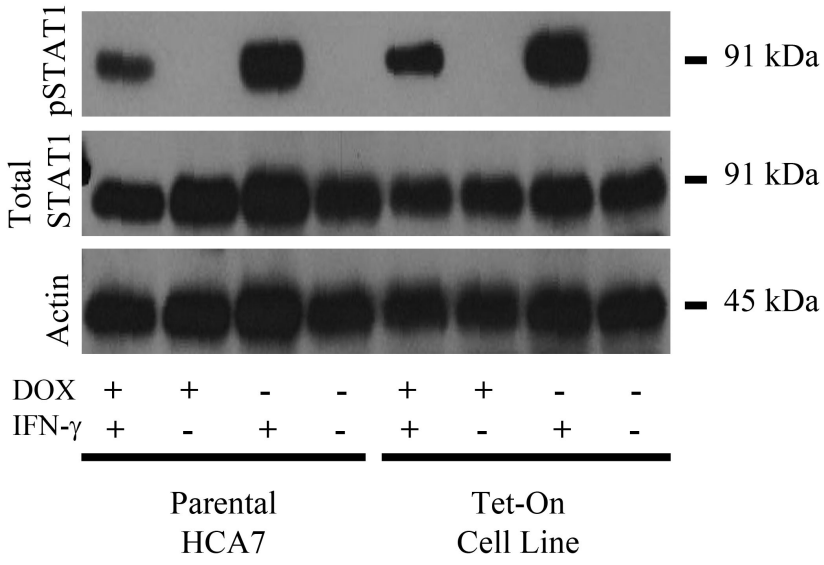
pSTAT1
Total STAT1
Actin
91 kDa
91 kDa
45 kDa
DOX + + - - + + - -
IFN-γ + - + - + - + -
Parental HCA7
Tet-On Cell Line

Figure 16 | Localization of Mutant PTPN2 Following IFN-γ Stimulation

C216S dominant negative cells and control tet expressing cells were seeded on glass slides and treated with doxycycline (15 μg/ml) to induce expression of the transgene, HA-C216S, prior to stimulation with IFN-γ (200U/ml) for 6 hours. Confocal imaging was used to assess localization of PTPN2 (green) in C216S cells to evaluate if the mutation caused any disturbances in TC45 trafficking. C216S expressing cells showed an increase in PTPN2 in the nucleus whereas PTPN2 in control cells appeared to remain cytoplasmic or perinuclear. However, striking increases in PTPN2 localization to the membrane are indeed observed in the right panel. HA (red) co-localizes with the PTPN2 in cells expressing the C216S mutant, indicating the location of the C216S mutant protein.

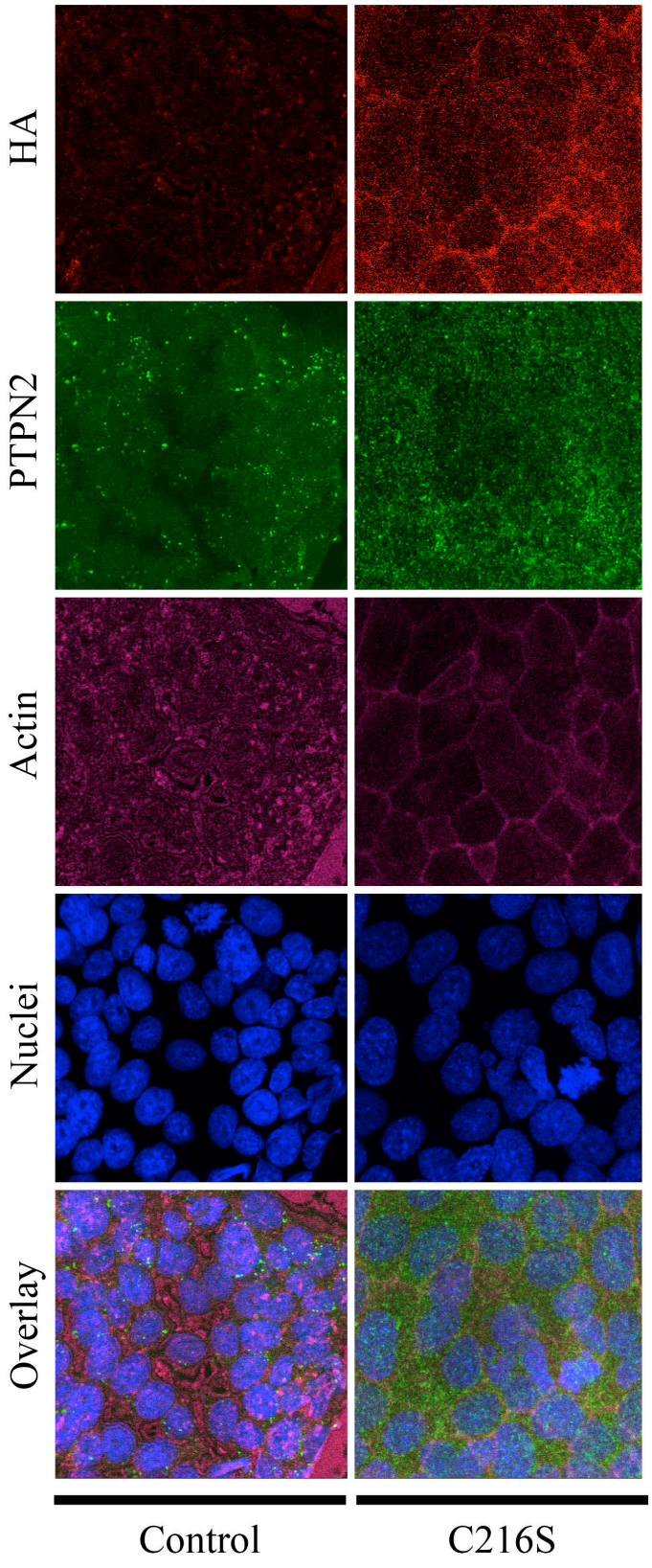
HA
PTPN2
Actin
Nuclei
Overlay
Control
C216S

Figure 17 | The Effect of TC45^{C216S} on Claudin-2 and Matriptase-1 Localization and Expression Following IFN-γ Stimulation

Confocal imaging was used to assess the trafficking and expression of claudin-2 following 6-hour IFN-γ stimulation [pre-treated for 48 hours with doxycycline (15 μg/ml)] within the mutant cell lines. An increase in claudin-2 (red) localized to the tight junctions is seen in the C216S mutants– where this pore-forming protein would be expected to exert its functional effects. A significant decrease in overall matriptase-1 (green) was observed in the C216S expressing cell lines. Furthermore, in control cells, matriptase-1 was, in large part, localized to the tight junctions whereas the mutant cell line shows only very low levels within the cytosol. The inverse relationship between CLD-2 and MAT-1 further supports the association of MAT-1 modulation of CLD2 with TC45 activity. In the overlay, Hoechst (blue) marks nuclear location and phalliodin (red) outlines the cellular membrane. Dr. Ronald Marchelletta is co-author with thesis author on material in his figure.

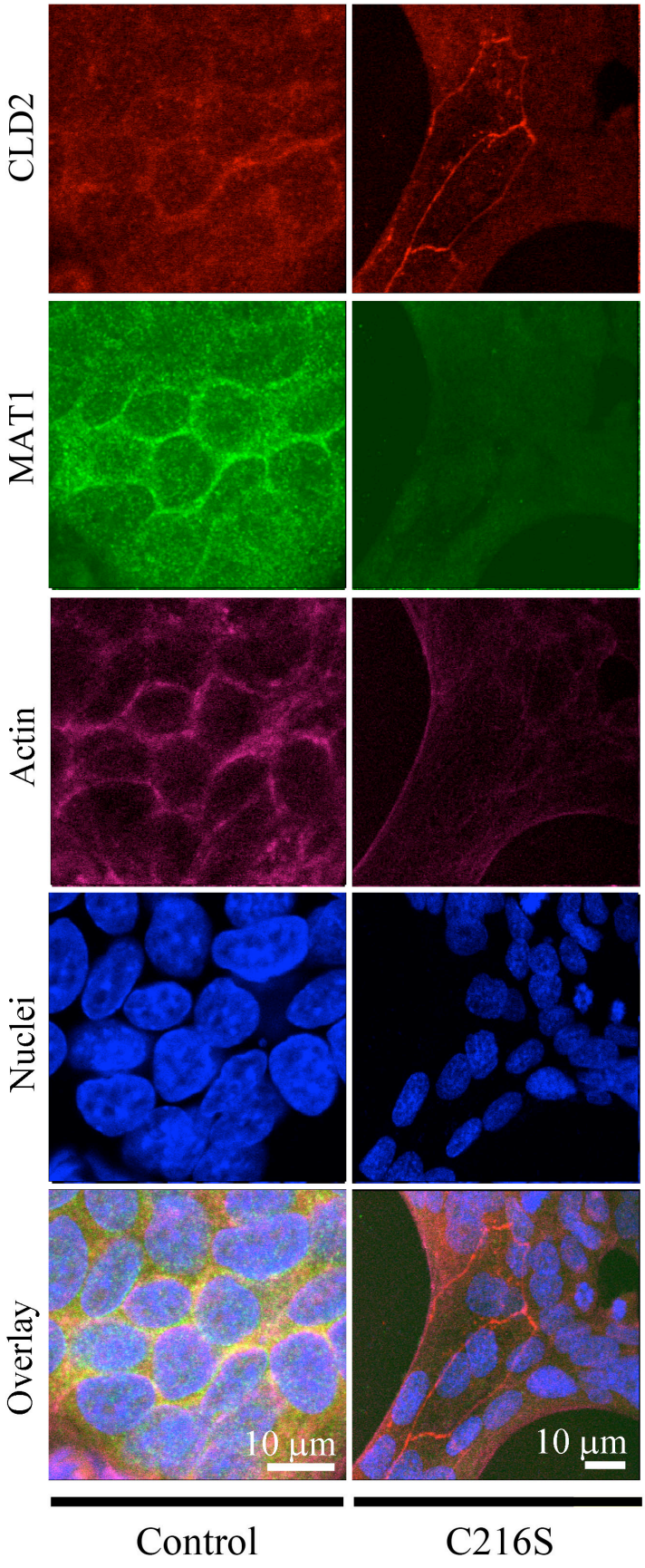
CLD2
MAT1
Actin
Nuclei
Overlay
10 µm
10 µm
Control
C216S

Figure 18 | The Effect of TC45^{C216S} Mutant on Claudin-2 and Matriptase-1 Protein Levels

C216S and tet expressing control cells were seeded on inserts and treated with doxycycline (15 μg/ml) 48 hours prior to IFN-γ stimulation. IFN-γ (200 U/ml) was added basolaterally to the inserts. Following 6 hours of incubation with IFN-γ, the cells were lysed to quantify levels of claudin-2 and matriptase-1. There was a significant increase in claudin-2 amounts observed in the C216S mutants compared to control (A). Concomitantly, a significant decrease in matriptase-1 is observed in the same C216S mutant cells compared to control (B). Both are shown in the representative western blot in the lower panel C. β-Actin was used throughout as a loading control. The relative protein level was assessed by densitometry (n = 4). Data are expressed as an average ± SEM. (*$P \leq 0.05$ compared to control cells, using Anova and the Student-Newman-Keuhls post-hoc test). Dr. Ronald Marchelletta is co-author with thesis author for material in this figure.

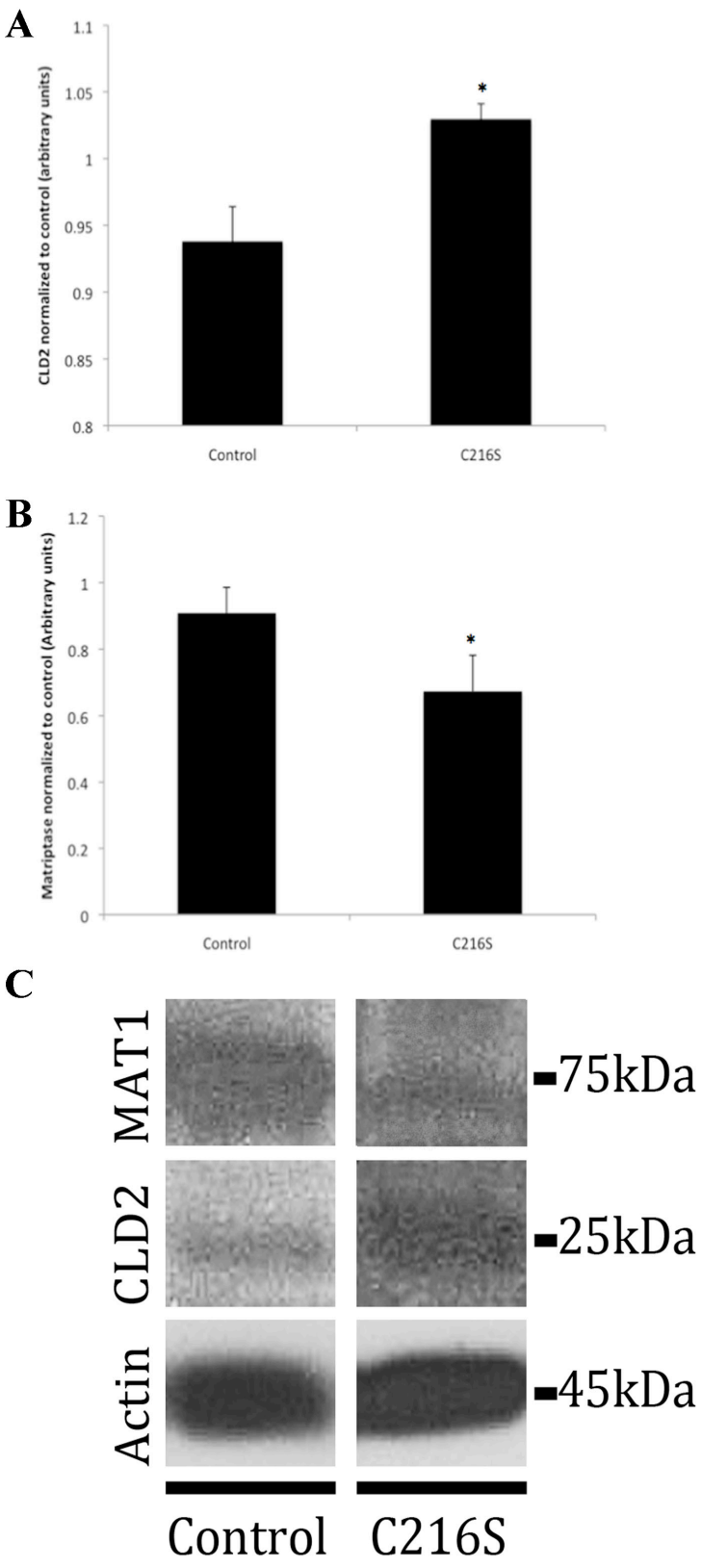
A
CLD2 normalized to control (arbitrary units)
1.1
1.05
1
0.95
0.9
0.85
0.8
*
Control
C216S
B
Matriptase normalized to control (Arbitrary units)
1.2
1
0.8
0.6
0.4
0.2
0
*
Control
C216S
C
MAT1
CLD2
Actin
75kDa
25kDa
45kDa
Control
C216S

Figure 19 | Serum Starvation Effects on Cell Line Disrupt Experiment

$TC45^{C216S}$ (C216S) and tet expressing (Control) cells were seeded ≈500,000 cells per 12 mm (0.6 cm^2 window area) insert. Transepithelial electrical resistance (TER) was monitored and normalized as $\Omega \cdot cm^2$. In order to observe the long-term effects of IFN-γ in the dominant negative cell line the cells were treated with DOX for 48 hours followed by 72 hours of IFN-γ treatment in which TER was monitored. Unfortunately, these cells exhibit a higher a metabolism and the effects of not changing the media for five days skewed the results. No trends were able to be observed.

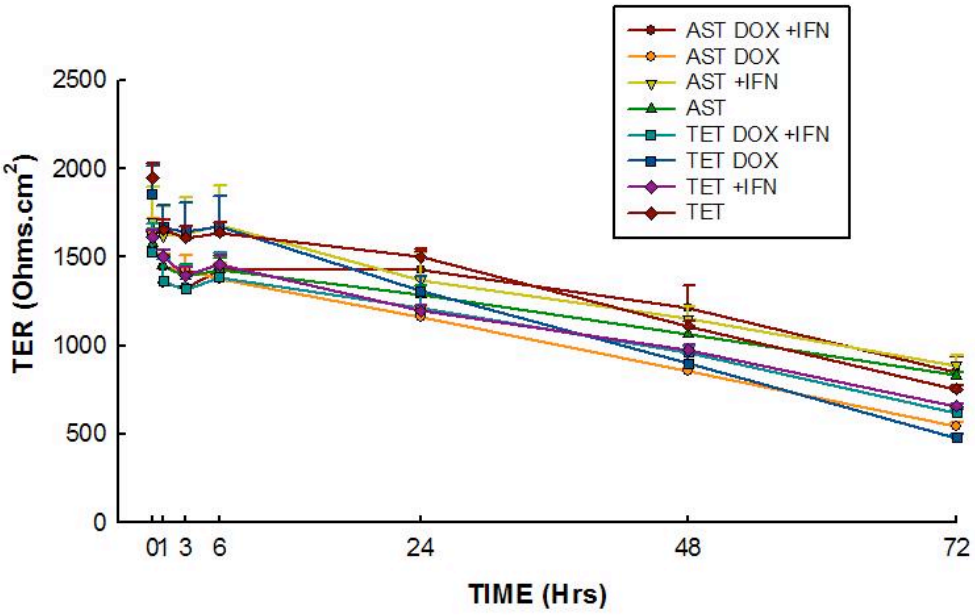
AST DOX +IFN
AST DOX
AST +IFN
AST
TET DOX +IFN
TET DOX
TET +IFN
TET
TER (Ohms.cm2)
2500
2000
1500
1000
500
0
01 3 6
24
48
72
TIME (Hrs)

Figure 20 | C216S-Expressing Cells show Increased Epithelial Barrier Resistance

$TC45^{C216S}$ (C216S) and tet expressing (Control) cells were seeded ≈500,000 cells per 12 mm (0.6 cm^2 window area) insert. Transepithelial electrical resistance (TER) was monitored and normalized as $\Omega \cdot cm^2$. Individual TER was normalized to baseline TER when treated with DOX and then averaged. Panel A shows the DOX and IFN-γ co-stimulated C216S inserts and control monitored for 48 hours after IFN-γ treatment. Panel B shows all conditions with DOX and IFN-γ co-stimulation, DOX alone, IFN-γ alone and untreated at 6 and 12 hours after treatment with IFN-γ. DOX shows a strong effect increasing the TER of both cell lines by 514 and 664 $\Omega \cdot cm^2$ for the co-stimulated mutant and control cell lines, respectively (Panel A). However, C216S cells were consistently observed to have reduced TER compared to control after treating with DOX, which triggers transcription of the mutant (treating with DOX). At 6 hrs, C216S expressing cells were 160 $\Omega \cdot cm^2$ lower than control, which was exaggerated to 216 $\Omega \cdot cm^2$ at the 12-hour time point post IFN-γ treatment. This represents a more compromised barrier in C216S expressing cells compared to control indicating C216S mutants decrease the protective effect of TC45 in maintaining barrier integrity.

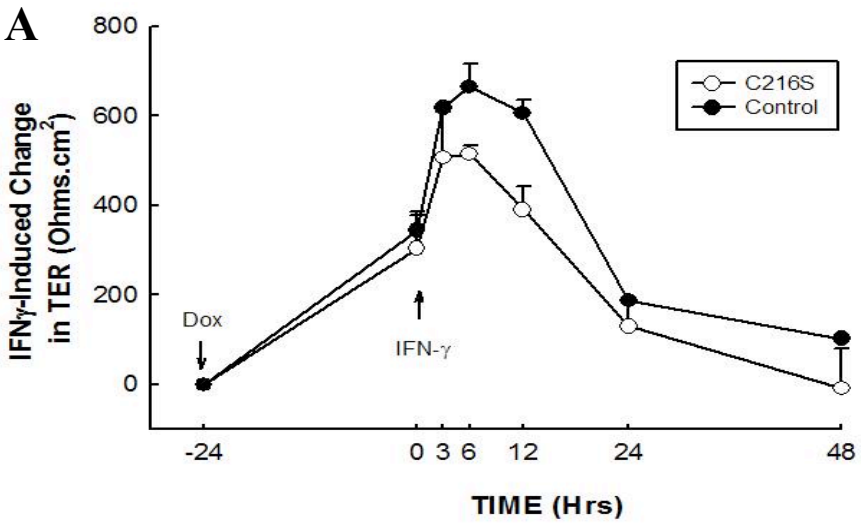
A
800
600
400
200
0
IFNγ-Induced Change in TER (Ohms.cm²)
C216S
Control
Dox
IFN-γ
-24
0 3 6
12
24
48
TIME (Hrs)

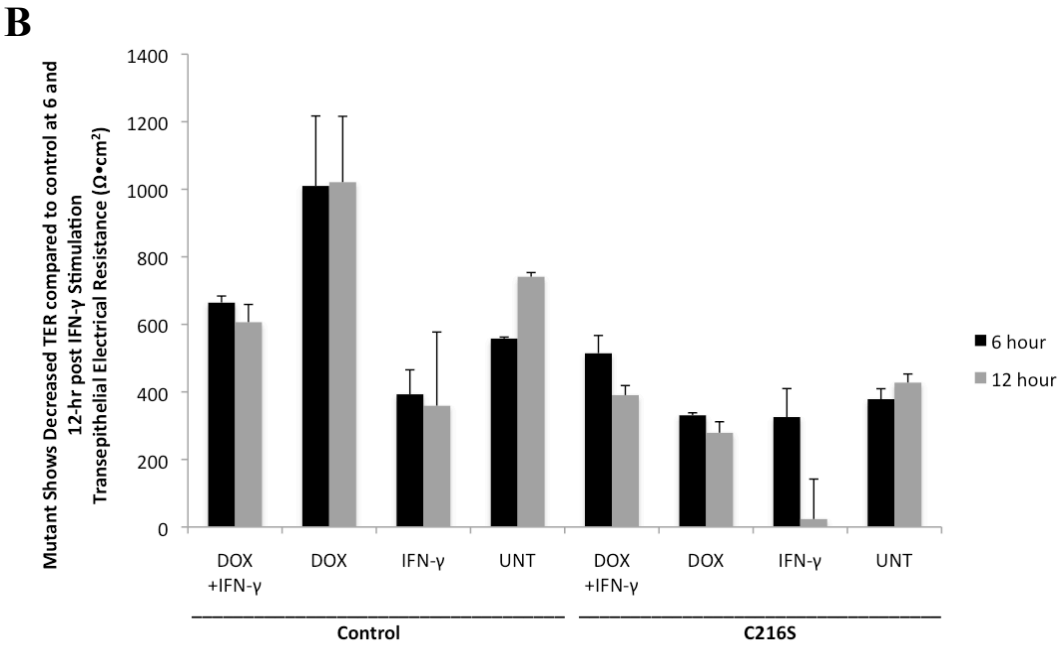
B
Mutant Shows Decreased TER compared to control at 6 and 12-hr post IFN-γ Stimulation
Transepithelial Electrical Resistance (Ω•cm²)
1400
1200
1000
800
600
400
200
0
6 hour
12 hour
DOX +IFN-γ
DOX
IFN-γ
UNT
DOX +IFN-γ
DOX
IFN-γ
UNT
Control
C216S

VI. TABLES

Table 1 | List of Primers

All primers were ordered from Integrated DNA Technologies (IDT) and reconstituted with DI water to a concentration of 100μM.

Type of Reactions	Name of Primer	Primer Sequence
CMV-HA Sequencing Forward	Core CMV primers	Provided by Core Facilities
CMV-HA Sequencing Reverse	Core CMV primers	Provided by Core Facilities
Mutagenesis Forward	For mutation	5'-GCC CGA ATT CGG TCA CCG AGA TC-3'
Mutagenesis Reverse	Rev mutation	5'-GAA TTC TGC AGT CCA CGG TAC CAC GC-3'
PCR BamHI site	TC45 PCROUT BamHI For	5'-CCT GGA GAA GGA TCC ATG TAC CCA GAT GTT-3'
PCR MluI Site	TC45 PCROUT MluI mut Rev	5'-TAA TTC ACG CGT GGT ACC GTG GAC TGC AGA ATT-3'
Lenti-X-HA vector Sequencing Forward	Lenti forward 1	5'-AGC AGA GCT CGT TTA GTG AAC CGT-3'
Lenti-X-HA vector Sequencing Reverse	PS4 R	5'-TCT CTT GGT CAT CTG TTG GCC-3'
Tet RTPCR Forward	Tet-on forward PS1	5'-ACA GAG TTC TTG AAG TGG TGG CCT-3'
Tet RTPCR Reverse	Tet-on Reverse PS1	5'-TGG TTT GTT TGC CGG ATC AAG AGC-3'

Table 2 | p24 ELISA Titers

Titering performed within Barrett/McCole using Lenti-X p24 Titer Kit. Absorbances were compared to a p24 standard curve. Calculations performed according to Clontech manual.

Virus	Titer by p24 ELISA
pLVX-Tet-On	$4.5x10^8$
pLVX-HA-TC45^{WT}	$1.6x10^8$
pLVX-HA-TC45^{C216S}	$2.0x10^8$
pLVX-HA-TC45$^{N206\text{-}fs}$	$7.0x10^8$

Table 3 | Core Facility Titers

UCSD core facilities titer counts provided. Colony forming units (CFU) was measured by HEK293 cells.

Virus	Titer (cfu/ml)
pLVX-Tet-On	$1.0x10^{9}$
pLVX-HA-TC45^{WT}	$5.0x10^{8}$
pLVX-HA-TC45^{C216S}	$5.5x10^{8}$

REFERENCES

1. JR Turner: Intestinal mucosal barrier function in health and disease. *Nature reviews. Immunology* 2009, 9:799-809.

2. MC Arrieta, L Bistritz, JB Meddings: Alterations in intestinal permeability. *Gut* 2006, 55:1512-20.

3. M Scharl, G Paul, A Weber, BC Jung, MJ Docherty, M Hausmann, G Rogler, KE Barrett, DF McCole: Protection of epithelial barrier function by the Crohn's disease associated gene protein tyrosine phosphatase n2. *Gastroenterology* 2009, 137:2030-2040 e5.

4. H Schmitz, C Barmeyer, AH Gitter, F Wullstein, CJ Bentzel, M Fromm, EO Riecken, JD Schulzke: Epithelial barrier and transport function of the colon in ulcerative colitis. *Annals of the New York Academy of Sciences* 2000, 915:312-26.

5. DC Baumgart, WJ Sandborn: Inflammatory bowel disease: clinical aspects and established and evolving therapies. *Lancet* 2007, 369:1641-57.

6. EV Loftus, Jr.: Clinical epidemiology of inflammatory bowel disease: Incidence, prevalence, and environmental influences. *Gastroenterology* 2004, 126:1504-17.

7. DK Podolsky: Inflammatory bowel disease. *N Engl J Med* 2002, 347:417-29.

8. SL Robbins, V Kumar, RS Cotran: Robbins and Cotran pathologic basis of disease, 8th edn. Philadelphia, PA: Saunders/Elsevier; 2010.

9. IJ Fuss, M Neurath, M Boirivant, JS Klein, C de la Motte, SA Strong, C Fiocchi, W Strober: Disparate CD4+ lamina propria (LP) lymphokine secretion profiles in inflammatory bowel disease. Crohn's disease LP cells manifest increased secretion of IFN-gamma, whereas ulcerative colitis LP cells manifest increased secretion of IL-5. *J Immunol* 1996, 157:1261-70.

10. CT Capaldo, A Nusrat: Cytokine regulation of tight junctions. *Biochimica et biophysica acta* 2009, 1788:864-71.

11. A Franke, T Balschun, TH Karlsen, J Hedderich, S May, T Lu, D Schuldt, S Nikolaus, P Rosenstiel, M Krawczak, et al: Replication of signals from recent studies of Crohn's disease identifies previously unknown disease loci for ulcerative colitis. *Nature genetics* 2008, 40:713-5.

12. KE You-Ten, ES Muise, A Itie, E Michaliszyn, J Wagner, S Jothy, WS Lapp, ML Tremblay: Impaired bone marrow microenvironment and immune function in T cell protein tyrosine phosphatase-deficient mice. *The Journal of experimental medicine* 1997, 186:683-93.

13. S Galic, M Klingler-Hoffmann, MT Fodero-Tavoletti, MA Puryer, TC Meng, NK Tonks, T Tiganis: Regulation of insulin receptor signaling by the protein tyrosine phosphatase TCPTP. *Molecular and cellular biology* 2003, 23:2096-108.

14. E Mattila, T Pellinen, J Nevo, K Vuoriluoto, A Arjonen, J Ivaska: Negative regulation of EGFR signalling through integrin-alpha1beta1-mediated activation of protein tyrosine phosphatase TCPTP. *Nature cell biology* 2005, 7:78-85.

15. T Yamamoto, Y Sekine, K Kashima, A Kubota, N Sato, N Aoki, T Matsuda: The nuclear isoform of protein-tyrosine phosphatase TC-PTP regulates interleukin-6-mediated signaling pathway through STAT3 dephosphorylation. *Biochemical and biophysical research communications* 2002, 297:811-7.

16. T Kisseleva, S Bhattacharya, J Braunstein, CW Schindler: Signaling through the JAK/STAT pathway, recent advances and future challenges. *Gene* 2002, 285:1-24.

17. J ten Hoeve, M de Jesus Ibarra-Sanchez, Y Fu, W Zhu, M Tremblay, M David, K Shuai: Identification of a nuclear Stat1 protein tyrosine phosphatase. *Molecular and cellular biology* 2002, 22:5662-8.

18. MH Lam, BJ Michell, MT Fodero-Tavoletti, BE Kemp, NK Tonks, T Tiganis: Cellular stress regulates the nucleocytoplasmic distribution of the protein-tyrosine phosphatase TCPTP. *J Biol Chem* 2001, 276:37700-7.

19. KA Mowen, J Tang, W Zhu, BT Schurter, K Shuai, HR Herschman, M David: Arginine methylation of STAT1 modulates IFNalpha/beta-induced transcription. *Cell* 2001, 104:731-41.

20. KM Heinonen, FP Nestel, EW Newell, G Charette, TA Seemayer, ML Tremblay, WS Lapp: T-cell protein tyrosine phosphatase deletion results in progressive systemic inflammatory disease. *Blood* 2004, 103:3457-64.

21. MS Buzza, S Netzel-Arnett, T Shea-Donohue, A Zhao, CY Lin, K List, R Szabo, A Fasano, TH Bugge, TM Antalis: Membrane-anchored serine protease matriptase regulates epithelial barrier formation and permeability in the intestine. *Proceedings of the National Academy of Sciences of the United States of America* 2010, 107:4200-5.

22. S Netzel-Arnett, MS Buzza, T Shea-Donohue, A Desilets, R Leduc, A Fasano, TH Bugge, TM Antalis: Matriptase protects against experimental colitis and promotes intestinal barrier recovery. *Inflamm Bowel Dis* 2012, 18:1303-14.

23. T Tiganis, BE Kemp, NK Tonks: The protein-tyrosine phosphatase TCPTP regulates epidermal growth factor receptor-mediated and phosphatidylinositol 3-kinase-dependent signaling. *J Biol Chem* 1999, 274:27768-75.

24. G Tiscornia, O Singer, IM Verma: Production and purification of lentiviral vectors. *Nat Protoc* 2006, 1:241-5.

25. J Lee, JH Mo, K Katakura, I Alkalay, AN Rucker, YT Liu, HK Lee, C Shen, G Cojocaru, S Shenouda, et al: Maintenance of colonic homeostasis by distinctive apical TLR9 signalling in intestinal epithelial cells. *Nature cell biology* 2006, 8:1327-36.

26. M Scharl, P Hruz, DF McCole: Protein tyrosine phosphatase non-receptor Type 2 regulates IFN-gamma-induced cytokine signaling in THP-1 monocytes. *Inflammatory bowel diseases* 2010, 16:2055-64.

27. RB Adams, SM Planchon, JK Roche: IFN-gamma modulation of epithelial barrier function. Time course, reversibility, and site of cytokine binding. *Journal of immunology* 1993, 150:2356-63.